70 (3) 133–165


# Detecting the basal dichotomies in the monophylum of carrion and rove beetles (Insecta: Coleoptera: Silphidae and Staphylinidae) with emphasis on the Oxyteline group of subfamilies

Vasily V. Grebennikov [1] & Alfred F. Newton [2]

[1] Ottawa Plant Laboratory, Canadian Food Inspection Agency, K.W. Neatby Bldg., 960 Carling Avenue, Ottawa, Ontario K1A 0C6, Canada [vasily.grebennikov@inspection.gc.ca]

[2] Field Museum of Natural History, 1400 South Lake Shore Drive, Chicago IL 60605–2496, USA [anewton@fieldmuseum.org]

*Received 19.iii.2012, accepted 05.xi.2012.*
*Published online at www.arthropod-systematics.de on 14.xii.2012.*

## > Abstract

Carrion beetles (Silphidae) and rove beetles (Staphylinidae, including Scaphidiinae, Pselaphinae and Scydmaeninae) form a well supported and exceptionally species-rich clade with nearly 58,000 described Recent species (of them Silphidae constitute 0.3%). The presently accepted classification implies a sister-group relationship between these families. The enormous clade of Staphylinidae, if indeed monophyletic, has its basal-most dichotomies inadequately hypothesized. We analysed 240 parsimony-informative larval and adult morphological characters for 34 terminals of carrion (3) and rove beetles (31) and rooted the obtained topologies on *Neopelatops* (Leiodidae). The most fully resolved topologies from the combined dataset consistently suggest that carrion and rove beetles are indeed monophyletic sister-groups. Two ancient species-poor rove-beetle subfamilies (Apateticinae with two genera in the eastern Palaearctic, and the monogeneric Holarctic Trigonurinae) branch off as a clade from the rest of Staphylinidae, rather than with members of the Oxyteline Group. Subsequent dichotomies of the staphylinid main clade remain obscure. A newly redefined and monophyletic Oxyteline Group is formed by Scaphidiinae + (Oxytelinae + Osoriinae + Piestinae), the last subfamily paraphyletic with respect to the previous two, which are monophyletic. The Oxyteline Group and the earlier detected monophyletic Omaliine and Staphylinine Groups form three main subdivisions within the rove beetles. Their interrelationships, as well as those with the possibly monophyletic Tachyporine Group (which includes the mega-diverse Aleocharinae), form the main unresolved questions in basal Staphylinidae phylogeny.

## > Key words

Trigonurinae, Apateticinae, Piestinae, Oxyporinae, Osoriinae, Scaphidiinae, taxonomy, phylogeny, classification, morphology.

## 1. Introduction

Carrion beetles (Silphidae) and rove beetles (Staphylinidae, incl. Scaphidiinae, Pselaphinae and Scydmaeninae) are easy-to-recognize and often highly visible actively feeding members of nearly all terrestrial biota (Sikes 2005; Thayer 2005). The two families together correspond approximately to the informal historical group "Brachelytra", a name referring to one of their more distinctive features (elytra more or less abbreviated and exposing part of the abdomen from above). These two families form a well supported and exceptionally species-rich clade with nearly 58,000 described species (of them only 186 Silphidae, constituting only about 0.3% of the total diversity) (Newton 2007, numbers updated through mid-2011). During


**Fig. 1.** Larval habitus of some terminal taxa included in the phylogenetic analysis. **A**: *Necrodes surinamensis* (Silphidae), USA, Maine; **B**: *Nicrophorus orbicollis* (Silphidae), USA, Alabama; **C**: *Lispinus* sp. (Osoriinae), Panama; **D**: *Thoracophorus sculptus* (Osoriinae), Australia; **E**: *Priochirus* sp. (Osoriinae), Mexico; **F**: *Glyptoma* sp. (Osoriinae), Mexico; **G**: *Piestus pygmaeus* (Piestinae), Mexico; **H**: *Siagonium punctatum* (Piestinae), USA, Arizona; **I**: *Hypotelus* sp. (Piestinae), Panama; **J**: *Eupiestus* sp. (Piestinae), Laos; **K**: *Prognathoides mjobergi* (Piestinae), Australia; **L**: *Bledius* sp. (Oxytelinae), Australia; **M**: *Ochthephilus planus* (Oxytelinae), USA, New Hampshire; **N**: *Anotylus rugosus* (Oxytelinae), Canada, Ontario; **O**: *Cyparium terminale* (Scaphidiinae), Mexico; **P**: *Scaphidium* sp. (Scaphidiinae), Panama. Scale bars 1 mm.

the last three decades, significant progress has been made in detecting phylogenetic events within Silphidae + Staphylinidae and using these results to modernize the classification of this group:

• LAWRENCE & NEWTON (1982) summarized the classification of Coleoptera at that time and proposed that the 22-odd staphylinid subfamilies recognized then could be organized into four main lineages or informal groups (Oxyteline, Omaliine, Tachyporine and Staphylinine Groups). They formally included several former families or silphid subfamilies in the Omaliine Group as staphylinid subfamilies (e.g., Microsilphinae, Empelidae, Dasyceridae), and suggested that several other then-recognized families (Pselaphidae, Scaphidiidae, Scydmaenidae and Silphidae) could belong within one or another of these groups of Staphylinidae.

• NEWTON & THAYER (1992), in a review of family-group names in Staphyliniformia with comments on classification, formally recognized Scaphidiinae as a staphylinid subfamily (first suggested by KASULE 1966, corroborated by LESCHEN & LÖBL 1995), recognized Apateticinae and Trigonurinae as subfamilies rather than tribes of Piestinae, and formally named Empelinae and Solieriinae as staphylinid subfamilies.

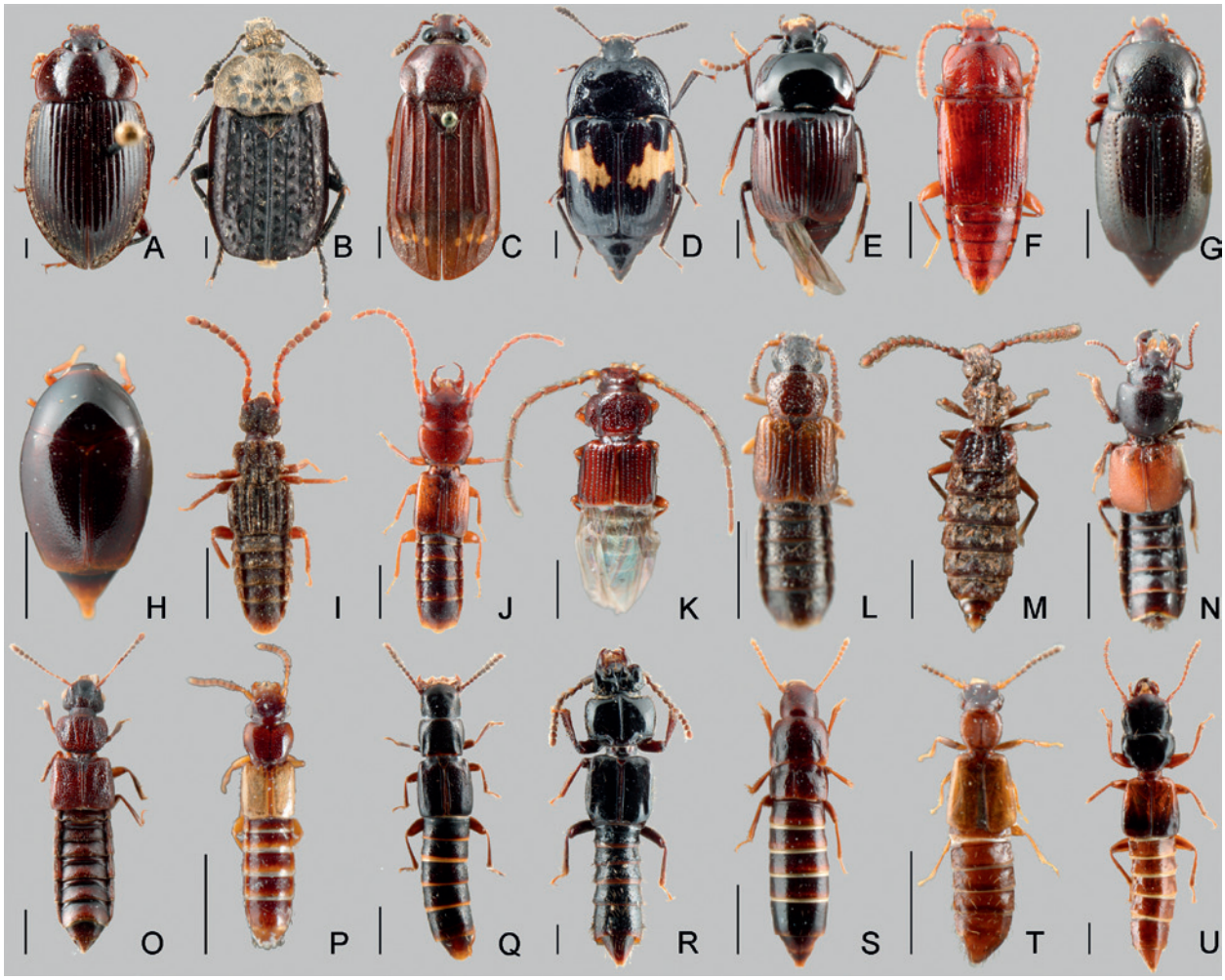


**Fig. 2.** Adult habitus of some terminal taxa included in the phylogenetic analysis. **A**: *Necrophilus hydrophiloides* (Agyrtidae), an out-group taxon, Canada, British Columbia; **B**: *Thanatophilus lapponicus* (Silphidae), Canada, Newfoundland; **C**: *Necrodes surinamensis* (Silphidae), USA, Kentucky; **D**: *Nodynus leucofasciatus* (Apateticinae), Japan; **E**: *Apatetica* sp. (Apateticinae), China, Yunnan; **F**: *Trigonurus crotchii* (Trigonurinae), Canada, British Columbia; **G**: *Scaphium castanipes* (Scaphidiinae), USA, Maine; **H**: *Scaphisoma castaneum* (Scaphidiinae), Canada, British Colombia; **I**: *Eupiestus feae* (Piestinae), Laos; **J**: *Siagonium quadricorne* (Piestinae), Czech Republic; **K**: *Piestus mexicanus* (Piestinae), Mexico; **L**: *Homalotrichus striatus* (Oxytelinae), Chile; **M**: *Oxypius peckorum* (Oxytelinae), Australia; **N**: *Bledius fortis* (Oxytelinae), USA, Texas; **O**: *Anotylus rugosus* (Oxytelinae), Hungary; **P**: *Hypotelus pusillus* (Piestinae), Mexico; **Q**: *Lispinus cordilliensis* (Osoriinae), Guatemala; **R**: *Priochirus japonicus* (Osoriinae), Japan; **S**: *Paratorchus* sp. (Osoriinae), New Zealand; **T**: *Renardia nigrella* (Osoriinae), Canada, British Columbia; **U**: *Eleusis capitata* (Osoriinae), Democratic Republic of Congo. Scale bars 1 mm.

• Ashe & Newton (1993) and Ashe (2005) focused on the phylogeny of the Tachyporine Group, although they did not test its monophyly.

• Newton & Thayer (1995) focused on the phylogeny of the Omaliine Group, ranking the former "family Pselaphidae" down to a subfamily nested well within a monophyletic Omaliine Group, and corroborated the placement of Microsilphinae, Glypholomatinae, Micropeplinae and Dasycerinae in this group.

• Newton (1997) formally revised the historically broad concept of the family Silphidae to exclude Agyrtidae, and placed (or corroborated the placement of) an assortment of other odd "silphid" groups or genera elsewhere, mostly in the families Leiodidae (e.g., Catopocerinae, Leptodirini, Estadiini, *Agyrtodes* Portevin, *Catopsolius* Broun, *Eupelates* Portevin and *Tricholoma* Hlisnikovský) or Staphylinidae (e.g., Apateticini, Glypholomatinae, Microsilphini, *Brathinus* LeConte, *Camioleum* Lewis, *Deinopteroloma* Jansson, *Empelus* LeConte and *Silphotelus* Broun), leaving only the subfamilies Nicrophorinae and Silphinae in Silphidae. Subsequent studies including the molecular phylogeny of Dobler & Müller (2000) have corroborated the monophyly of Silphidae in this sense and of its two subfamilies, and confirmed the exclusion of Agyrtidae from Silphidae and its close relationship to Leiodidae.

• Hansen (1997), Beutel & Molenda (1997), Beutel & Leschen (2005), Caterino et al. (2005), Hunt et al. (2007) and Lawrence et al. (2011), using diverse morphological and molecular data in broad phylogenetic studies including at least all major sub-groups of Staphylinoidea, demonstrated anew the monophyly of Silphidae + Staphylinidae (excluding Agyrtidae), although relationships among the groups within this monophylum varied among these studies.
• Thayer (2005) summarized the rove-beetle classification at that time and presented a summary diagram of phylogenetic relationships among the subfamilies based on studies up to that time (diagram updated in Newton 2011).
• Grebennikov & Newton (2009) focused on the phylogeny of the Staphylinine Group, ranking the former "family Scydmaenidae" down to a subfamily nested well within a monophyletic Staphylinine Group; the family Silphidae, suggested as a possible member of this group by Lawrence & Newton (1982), was included in their analysis but excluded from the group and retained as a family separate from Staphylinidae.

The Oxyteline Group is the only one of the four large putative staphylinid lineages whose monophyly and internal relationships have not been the subject of recent focused study. This group of six subfamilies (Apateticinae, Trigonurinae, Oxytelinae, Piestinae, Osoriinae, Scaphidiinae; see Thayer 2005) is the smallest of the four lineages with "only" 5943 described species, placed in about 215 genera. The species are small to moderate in size (ca. 1–10 mm long), variable in shape (e.g., Fig. 2D–U), found in diverse habitats but often associated with decaying trees or other decaying matter, and are biologically exceptional within Staphylinidae in being, as far as known, entirely saprophagous or (Scaphidiinae) mycophagous rather than carnivorous like the great majority of species in the other three staphylinid groups. Although subfamily interrelationships have not been addressed, several phylogenetic studies have been conducted on or within the larger subfamilies. Oxytelinae was demonstrated as monophyletic by Herman (1970), notably by their common possession of a unique pair of defensive glands at the abdominal apex, and phylogenetic relationships among the oxyteline tribes and genera were initiated in that study and partially extended by Newton (1982) and Makranczy (2006). The monophyly and internal relationships among tribes and genera of Scaphidiinae were explored by Leschen & Löbl (1995). Piestinae, even after removal of the tribes Apateticini and Trigonurini as separate subfamilies by Newton & Thayer (1992) based on larval characters indicated in Newton (1982), has not been demonstrated as monophyletic. A phylogenetic study of *Piestus* Gravenhorst species by Caron et al. (2012) that included as out-group taxa representatives of all six other piestine genera did find support for monophyly of that large genus and for relationships among the genera. Lastly, Irmler (2010), in a cladistic analysis of a majority (24 out of 36) of genera of the osoriine tribe Thoracophorini, found support for the monophyly of this tribe but not for some of the included subtribes.

Our original goals in this study were thus (1) to test the monophyly of all non-monogeneric subfamilies constituting the so-called "Oxyteline Group" of rove-beetle subfamilies and (2) to test the monophyly of the Oxyteline Group and hypothesize its sister-group relationships among other deeply-rooted Staphylinidae clades. As our work progressed, preliminary results indicated that the Oxyteline Group, as delimited above, is likely a polyphyletic assemblage consisting of at least two, possibly three monophyletic subunits. Of them the largest was thought to be the Oxyteline Group *sensu stricto* (comprised of Oxytelinae, Piestinae, Osoriinae and likely Scaphidiinae), while the remaining subfamilies, Apateticinae and Trigonurinae, were suspected of having originated from the one or two basal-most dichotomies within the family. These preliminary findings were not completely novel: Apateticinae and Scaphidiinae had also been placed outside the Oxyteline Group (as separate families) in Hansen (1997), although without strong support, and Madge (1980) had earlier argued strongly that Apateticinae and Trigonurinae belong in Silphidae rather than Staphylinidae. We, therefore, widened the scope of our work with the goal (3) to test and document these alternative hypotheses of the composition of the Oxyteline Group and of Silphidae. This necessitated adding into the in-group representatives of Silphidae, a supposed monophylum presently conventionally seen as the likeliest sister-group of Staphylinidae, if not a member of it, but with an old history of confusing and shifting taxonomic limits (see Newton 1997).

## 2. Material and methods

### 2.1. Choice of in-group and out-group taxa

Representatives of all rove-beetle subfamilies currently assigned to the Oxyteline Group (Apateticinae, Trigonurinae, Oxytelinae, Piestinae, Osoriinae, Scaphidiinae; see Thayer 2005) were included in the analysis (Table 1; see also Appendix 2, and Figs. 1 and 2 for habitus of selected larvae and adults). Place-

**Table 1.** List of 36 terminals (genera) included into the phylogenetic analysis to detect the basal-most Staphylinidae + Silphidae dichotomies and composition of the Oxyteline Group of the rove-beetle subfamilies. All but two Staphylinidae subfamilies are grouped in four informal groups: Oxyteline Group (OxGr), Tachyporine Group (TaGr), Omaliine Group (OmGr) and Staphylinine Group (StGr). "Subfamily Piestinae" is non-monophyletic and the traditional name is used for convenience only. Both adult and larval morphological characters were studied for all terminals, although not always for the same species.

| Family | Group | Subfamily | Genus |
|---|---|---|---|
| LEIODIDAE | n/a | CAMIARINAE | *Neopelatops* Jeannel, 1936 |
| AGYRTIDAE | n/a | NECROPHILINAE | *Necrophilus* Latreille, 1829 |
| SILPHIDAE | n/a | SILPHINAE | *Thanatophilus* Leach, 1815 |
| SILPHIDAE | n/a | SILPHINAE | *Necrodes* Leach, 1815 |
| SILPHIDAE | n/a | NICROPHORINAE | *Nicrophorus* Fabricius, 1775 |
| STAPHYLINIDAE | n/a | TRIGONURINAE | *Trigonurus* Mulsant, 1847 |
| STAPHYLINIDAE | n/a | APATETICINAE | *Apatetica* Westwood, 1848 |
| STAPHYLINIDAE | n/a | APATETICINAE | *Nodynus* Waterhouse, 1876 |
| STAPHYLINIDAE | OxGr | "PIESTINAE"" | *Piestus* Gravenhorst, 1806 |
| STAPHYLINIDAE | OxGr | "PIESTINAE"" | *Siagonium* Kirby & Spence, 1815 |
| STAPHYLINIDAE | OxGr | "PIESTINAE"" | *Hypotelus* Erichson, 1839 |
| STAPHYLINIDAE | OxGr | "PIESTINAE"" | *Eupiestus* Kraatz, 1859 |
| STAPHYLINIDAE | OxGr | "PIESTINAE"" | *Prognathoides* Steel, 1950 |
| STAPHYLINIDAE | OxGr | OXYTELINAE | *Oxypius* Newton, 1982 |
| STAPHYLINIDAE | OxGr | OXYTELINAE | *Homalotrichus* Solier, 1849 |
| STAPHYLINIDAE | OxGr | OXYTELINAE | *Bledius* Leach, 1819 |
| STAPHYLINIDAE | OxGr | OXYTELINAE | *Ochthephilus* Mulsant & Rey, 1856 |
| STAPHYLINIDAE | OxGr | OXYTELINAE | *Anotylus* Thomson, 1859 |
| STAPHYLINIDAE | OxGr | OSORIINAE | *Renardia* Motschulsky, 1865 |
| STAPHYLINIDAE | OxGr | OSORIINAE | *Eleusis* Laporte, 1835 |
| STAPHYLINIDAE | OxGr | OSORIINAE | *Lispinus* Erichson, 1839 |
| STAPHYLINIDAE | OxGr | OSORIINAE | *Thoracophorus* Motschulsky, 1837 |
| STAPHYLINIDAE | OxGr | OSORIINAE | *Paratorchus* McColl, 1985 |
| STAPHYLINIDAE | OxGr | OSORIINAE | *Priochirus* Sharp, 1887 |
| STAPHYLINIDAE | OxGr | OSORIINAE | *Glyptoma* Erichson, 1839 |
| STAPHYLINIDAE | OxGr | SCAPHIDIINAE | *Scaphium* Kirby, 1837 |
| STAPHYLINIDAE | OxGr | SCAPHIDIINAE | *Scaphisoma* Leach, 1815 |
| STAPHYLINIDAE | OxGr | SCAPHIDIINAE | *Cyparium* Erichson, 1845 |
| STAPHYLINIDAE | OxGr | SCAPHIDIINAE | *Scaphidium* Oliver, 1790 |
| STAPHYLINIDAE | TaGr | TACHYPORINAE | *Tachinus* Gravenhorst, 1802 |
| STAPHYLINIDAE | TaGr | ALEOCHARINAE | *Drusilla* Leach, 1819 |
| STAPHYLINIDAE | OmGr | GLYPHOLOMATINAE | *Glypholoma* Jeannel, 1962 |
| STAPHYLINIDAE | OmGr | OMALIINAE | *Acrolocha* Thomson, 1858 |
| STAPHYLINIDAE | StGr | OXYPORINAE | *Oxyporus* Fabricius, 1775 |
| STAPHYLINIDAE | StGr | STENINAE | *Stenus* Latreille, 1797 |
| STAPHYLINIDAE | StGr | PSEUDOPSINAE | *Pseudopsis* Newman, 1839 |

ment of taxa below subfamily (e.g., to tribe or subtribe when used) is not indicated in Table 1 or Appendix 2, but can be found, e.g., in Newton & Thayer (2005). We also included representatives of Silphidae, which forms a clade with the family Staphylinidae *sensu latissimo* (i.e., including the subfamily Scydmaeninae; see Grebennikov & Newton 2009) and is conventionally treated as an independent family. Whenever possible, the morphological matrix includes three or more representatives from different genera of each in-group family/subfamily, thus allowing a partial test of their monophyly (except for the monogeneric Trigonurinae).

In order to rigorously test monophyly of the Oxyteline Group and suggest its sister-group, we included representatives of some rove-beetle subfamilies maintained outside of the Oxyteline Group (Thayer 2005), such as Glypholomatinae, Omaliinae, Tachyporinae, Aleocharinae, Oxyporinae, Steninae and Pseudopsinae (Table 1), thus including two or more subfamilies from each of the other three main staphylinid lineages.

A representative of Agyrtidae (*Necrophilus* Latreille, 1829) was included as a partial test for Staphylinidae + Silphidae monophyly. This relationship is otherwise strongly supported (see Beutel & Leschen 2005 and Lawrence et al. 2011), accepted by us as an

*a priori* underlying hypothesis, and, therefore, not explicitly tested in our analyses.

All obtained trees were rooted at *Neopelatops* Jeannel, 1936 (Leiodidae). Leiodidae is another family of the Staphylinoidea, see Fig. 4 for its likely phylogenetic position.

## 2.2. Sources of specimens, their identification, preparation and illustration

Lists of newly studied larval and adult specimens used in this work and their label data are provided in Appendix 2. Most specimens studied originated from the collection of the Division of Insects, Field Museum of Natural History, Chicago (FMNH); a few larval specimens were from the Canadian National Collection of Insects, Arachnids and Nematodes, Ottawa (CNC).

Identifications were made by A. Newton. Even though in larvae an exact determination of the instar is not always possible, we believe that only older-instar larvae were used to score characters, and we assume that comparing characters is legitimate even if possibly scored for different older instars. In most cases larvae were not reared from eggs in a laboratory, but collected in the field and identified to species using a combination of two main criteria: (1) repeated association records with the presumably conspecific adults and (2) underlying knowledge of larval morphology of Staphylinoidea, their distribution, biology, and habitat preferences. Conspecifity of *Apatetica* sp. larvae (described in Appendix 3; two specimens, GenBank accession numbers JX488294, JX488295) and adults (one specimen, JX488296) collected in the same sample was corroborated by comparing the 407 base pair "genetic barcoding" part of the CO1 gene and finding only two bases difference between two identical larval sequences and that of the adult.

Preparation of the adult and larval specimens for morphological study included macerating non-sclerotized tissue in hot 10% solution of KOH (thus clearing the cuticle) and, for some specimens, subsequent staining with chlorazol black. Specimens were mounted in Euparal on microscope slides and studied under dissecting and compound microscopes. Some adult specimens were partly disarticulated, allowing for free manipulation and rotation of the body parts, and stored in glycerol on microscope slides.

Photo images were taken with a Nikon DXM1200F digital camera attached to a Nikon SMZ1500 dissecting microscope at CNC (Figs. 1–5, 8) or with a Microptics ML Macro XLT digital system at FMNH (Figs. 9–11); those of Fig. 6 were provided by Artem Zaitsev (Moscow, Russia). Line drawings (Fig. 7) from slide-mounted larvae were prepared using a camera lucida attached to a compound microscope.

## 2.3. Morphological datasets and analysis

Two hundred sixty morphological characters were selected for the analysis; their description and state definitions are given in Appendix 1. The combined larval and adult morphological matrix includes 36 terminals and all 260 characters (Table 2); there are 10,140 cells, none of them polymorphic, 421 cells (4% of the matrix) with no data (66 because of lacking knowledge; 355 because of inapplicability of the character to the taxon). Characters 1–84 refer to larval morphology; characters 85–260 refer to adult morphology.

Each author was responsible for scoring one dataset (larval by VVG and adult by AFN), thus minimizing possible bias. The exact wording of all characters was then reviewed by both authors and changes were made to reach a consensus.

Both larval and adult morphological data were scored, in most of the cases, for the same species. In cases where this was impossible because of material limitation, different congeneric species were used. A few "chimera" terminals were thus created when these non-conspecific datasets were merged. It is assumed, however, that in such cases these species are more closely related to one another than to any other terminal in the same matrix and, therefore, larval and adult datasets might be merged without creating a phylogenetic conflict on incompatible terminals.

Twenty characters (26, 53, 100, 103, 111, 119, 120, 128, 132, 141, 150, 156, 157, 169, 195, 204, 213, 253, 255, 259) are parsimony-uninformative and were deactivated before analyses. Sixty one multi-state characters (2, 4, 5, 11, 15, 18, 20, 21, 22, 24, 25, 29, 31, 32, 36, 42, 45, 46, 51, 54, 56, 60, 64, 66, 68, 69, 71, 74, 77, 78, 79, 80, 81, 82, 83, 84, 86, 95, 97, 98, 105, 114, 122, 126, 127, 136, 139, 140, 147, 153, 160, 185, 191, 205, 206, 207, 208, 209, 210, 227, 241) were analysed as being either ordered (analyses 3, 4, 7, 8, 11, 12; Table 3) or unordered (analyses 1, 2, 5, 6, 9, 10; Table 3); all other multi-state characters were treated as unordered in all analyses.

We analysed three different morphological datasets: larval (characters 1–84; of them 82 are parsimony-wise informative), adult (characters 85–260; of them 158 are parsimony-wise informative), and combined (characters 1–260; of them 240 are parsimony-wise informative) using for each of them four possible combinations of ordering and weighting parameters. In total, 12 separate analyses of morphology data were implemented, and summarized in Table 3.

Three software packages were applied to the morphological data. Hennig86 (Farris 1988) was used to search for the shortest (= most parsimonious) trees (single heuristic search; commands "mh*" and "bb*") and then to perform successive approximations (Farris 1969; executed by a string of commands "xs w", "mh*" and "bb*" repeated in cycles until the tree statistics stabilized). Branch support in each particular analysis was assessed using Nona 2.0 (Goloboff 1999) through bootstrapping 1000 randomly generated trees. Winclada (Nixon 2002) was used as a shell program to construct the matrix and to communicate with both Hennig86 and Nona.

We use two statistical measures to assess our results numerically; both were first introduced in our earlier work on the Staphylinine Group of rove-beetle subfamilies (Grebennikov & Newton 2009), are expressed as a percentage, and are explained in the legend of Table 3. To judge the support of a particular clade across all analyses we employ the "Relative Support Value" (RSV). To compare the capacity of a particular analysis to resolve the Oxyteline Group and its subordinate clades (as resulting from analysis 9) we calculate a "Relative Resolution Value" (RRV). The RRV needs a reference topology; we choose the strict consensus tree of analysis #9 (Fig. 3) since this analysis is among the four most inclusive (larvae + adults; analyses #9 – 12) and among the latter is the most conservative (all characters unordered and equally weighted).

## 3. Results of the cladistic analyses

The results of the 12 parsimony analyses of morphological data are summarized in Table 3. Figure 3 is one among four most parsimonious trees from the combined larval and adult analysis #9 (Table 3) with unambiguously optimized evolutionary events plotted on internodes. Figure 4 is the consensus subfamily-level tree, representing the results of the present study and also summarizing present-day knowledge on the main clades within the superfamily Staphylinoidea based on the prior phylogenetic studies mentioned in the Introduction.

The four most parsimonious trees from the most conservative analysis #9 vary only in how the members of non-monophyletic "Piestinae" are scattered within the clade of "Piestinae" + Osoriinae + Oxytelinae, both latter subfamilies monophyletic. Re-weighting characters with successive approximation (analysis #10) resulted in the same four trees. Analyses #11 and #12 with the multi-state characters ordered and either weighted by successive approximation or not (Table 3) consistently failed to detect four clades recognized in the analyses #9 and #10: (1.) Oxyteline Group, (2.) Apateticinae + Trigonurinae, (3.) Staphylinidae excepting Apateticinae + Trigonurinae, as well as (4.) Staphylinidae excepting Apateticinae, Trigonurinae and Oxyteline Group. Bootstrap support for all clades (except Scaphidiinae) detected in the analyses with some multi-state characters ordered (analyses #11 and #12) was consistently lower, as compared to analyses #9 and #10 having all multi-state characters unordered (Table 3). Overall all 12 analyses could be judged as relatively congruent in their results with parts of their topologies frequently matching those on the reference tree (strict consensus of analysis #9).

Among the four subfamilies composing the Oxyteline Group *sensu stricto* (Osoriinae, Oxytelinae, Piestinae, Scaphidiinae) three were found to be likely monophyletic with the Relative Support Value (RSV) varying widely. Scaphidiinae was the most consistently recovered clade (RSV 88%), Osoriinae were moderately supported (RSV 46%), while Oxytelinae were weakly supported (RSV 17%). The "subfamily Piestinae" was never recovered as a clade (RSV 0%). Monophyly of the entire Oxyteline Group was weakly supported (RSV 25%). Within this clade, Scaphidiinae formed the sister-group to the weakly supported monophyletic rest (Osoriinae + Piestinae + Oxytelinae, RSV 29%), which, in turn, remained unresolved. The Oxyteline Group formed the sister to a weakly supported monophylum of Staphylinine Group + Omaliine Group + Tachyporine Group (RSV 17%).

Outside the Oxyteline Group, the subfamily Apateticinae comprising two genera has been recovered as a strongly supported clade (RSV 83%). It was grouped as sister to the monogeneric Trigonurinae into a moderately supported clade (RSV 38%). The sister-group of this clade was a weakly-to-moderately supported monophyletic rest of the family Staphylinidae. Both Staphylinidae and Silphidae were recovered as moderately supported clades with RSV 62% and 66%, respectively.

A small number of obtained trees contained groupings acutely conflicting with the most consistently resolved topology outlined above and depicted on Figs. 3, 4. Thus we recovered two clades, each weakly supported (RSV 17%), suggesting that (A) Silphidae without *Nicrophorus* cluster with Apateticinae and Trigonurinae and that (B) Scaphidiinae form a sister-group to the monophyletic rest of Staphylinidae. None among the recovered trees contained all three included Silphidae genera forming a clade with either Apateticinae or with Apateticinae and Trigonurinae.

**Table 2.** Data matrix of larval (1–84) and adult (85–260) morphological characters used for the phylogenetic analysis of the Oxyteline Group of the rove-beetle subfamilies (Coleoptera: Staphylinidae). Symbol 'N' in the bottom row indicates parsimony-wise uninformative characters deactivated before analyses; symbol 'O' indicates multi-state characters.

| | | | | | | | |
|---|---|---|---|---|---|---|---|
| | **0000000000000000000** | **0000000000000000000** | **0000000000000000000** | **0000000000000000000** | **0000000000000000001** | **1111111111111111111** | **1111111111** |
| | **0000000011111111112** | **2222222233333333334** | **4444444455555555556** | **6666666677777777778** | **8888888899999999990** | **0000000011111111112** | **2222222223** |
| | **1234567890123456789O** | **1234567890123456789O** | **1234567890123456789O** | **1234567890123456789O** | **1234567890123456789O** | **1234567890123456789O** | **1234567890** |
| *Neopelatops* | 0601001111000-300002 | 00-0000-101300010110 | 10012011010001001001 | 01020201001202010000 | 00001200001110200011 | 00001021110100001110 | 0-01110100 |
| *Necrophilus* | 0611001111000-200002 | 00-0000-101300010110 | 10012011010011121001 | 01020202002203010000 | 00001100001000200011 | 20012021110100001010 | 0-00110100 |
| *Thanatophilus* | 16001010101010100002 | 0200100-102300020011 | 11001010010101121002 | 01020002012203011000 | 00001110110010200011 | 20012121110100001110 | 0-11110100 |
| *Necrodes* | 06001010101010100002 | 0200100-202200020111 | 11001010010101121002 | 01020002012203011000 | 00001110110010200011 | 20011121110100001110 | 0-11110100 |
| *Nicrophorus* | 0000000-100010200002 | 0200100-201200010000 | 10100010010001001002 | 01020100101201010000 | 00001210111010200101 | 21012121110100001110 | 0-10110100 |
| *Trigonurus* | 16111010100010100102 | 1211000-002300010110 | 22101010012000101000 | 01010002002203l0???? | ????0010001100200001 | 20000-01110100001010 | 0-01010100 |
| *Apatetica* | 16111010100010100202 | 0200200-002300010000 | 11001000012000001001 | 01020000002103111110 | 00001200000000200001 | 20011021100110001010 | 1100110100 |
| *Nodynus* | 16111010100010100202 | 0200200-001400010000 | 21001010012001001001 | 01020000102202111100 | 00001110100000200001 | 20011021100110001010 | 1100110100 |
| *Piestus* | 04011010100010001002 | 0100100-101300010000 | 02101100012000001002 | 00021000102212010000 | 00002100000000201001 | 21010-01100210001111 | 0-00010100 |
| *Siagonium* | 04011010100010001002 | 0100100-101100010000 | 22100100012000001002 | 00121000102211010000 | 00002000000000201001 | 21010-01100210000210 | 1001000100 |
| *Hypotelus* | 01111010100010011002 | 1100100-101101110000 | 02101100012000001002 | 00021010102111010000 | 00002000100000200101 | 21010-01100110001010 | 0-01000100 |
| *Eupiestus* | 02011011100010001101 | 0200100-101100010000 | 02101100012000001002 | 00020000102211010000 | 00002100110000200101 | 21010-00110210001110 | 0-01000100 |
| *Prognathoides* | 03011010102010011002 | 0100100-102300020000 | 02101000011100001002 | 00021000202112010000 | 00002000110000200l? | 21010-01100210000110 | 0-01000101 |
| *Oxypius* | 1401101?100?10?????2 | 1100100-101201010000 | 01000100?2002001002 | 00021000102113011000 | 00002100101000210101 | 11010-01100210001010 | 0-01100100 |
| *Homalotrichus* | 00021???????????????1 | 0100100-100300010000 | 02101100012100001001 | 0002?00020010000---- | ----2100100000200101 | 21010-01100210001110 | 0-01000100 |
| *Bledius* | 03011110100110011000 | 2100100-101300010000 | 11000010002001001002 | 00021110100111011000 | 00002200001000210101 | 21110-01100210001110 | 0-00010100 |
| *Ochthephilus* | 03011010100010011101 | 0110100-101100010000 | 02100000012002001002 | 00021000202111010000 | 00002100111000210101 | 21010-01100210001210 | 0-01010100 |
| *Anotylus* | 01021010100110011000 | 1200100-101100010000 | 02101000012103001001 | 00021000101111011000 | 00002100110000210101 | 21010-01100210001210 | 0-00010100 |
| *Renardia* | 010110100---11011102 | 0110100-101101010000 | 01101100012000001102 | 00121000102111010000 | 00002101100000201211 | 21010-01100210000110 | 0-01021101 |
| *Eleusis* | 010110100---11011101 | 0110100-101201110000 | 02101000012000001102 | 00021000102111O????? | ????2000100000201211 | 21010-01110210001110 | 0-01021101 |
| *Lispinus* | 04010011102010011102 | 0100100-101400020000 | 03101100012100011102 | 00021000102111010000 | 00002100000000201111 | 21010-01100210001010 | 1001010101 |
| *Thoracophorus* | 03021010102010011101 | 0100100-101100010000 | 02100100002100001101 | 00121000102111010000 | 00002110100000211111 | 21010-01100210001010 | 1001000100 |
| *Paratorchus* | 01021011101010001000 | 21001110011420020000 | 01100200012000001002 | 1002?01020021100---- | ----2100000000111111 | 21010-00000010101210 | 0-01110111 |
| *Priochirus* | 00011011101010011001 | 0100100-102400010010 | 02101000012100011102 | 0002?002102111010000 | 00002100110000201001 | 21010-01110210001210 | 0-01000100 |
| *Glyptoma* | 0001??0-0---0-011002 | 1100100-001100000000 | 02100200012100001101 | 00021000102100010000 | 00002100110000202011 | 21010-01100210001010 | 0-01001101 |
| *Scaphium* | 05010110100010001002 | 12100011201100010000 | 01100010012101000O0- | --02000010121101l000 | 00001200101000201101 | 21001021010110101110 | 0-01110100 |
| *Scaphidium* | 05011010100010001002 | 11000011202400020000 | 02100010012001011002 | 00020000102211011111 | 11111200101001200101 | 21011021000000101110 | 0-01110100 |
| *Cyparium* | 05011010100010001002 | 12000010100100000000 | 02101010012002000O0- | --01001010111000---- | ----1200101001200101 | 21011021010110111110 | 0-01110100 |
| *Scaphisoma* | 05010110100010011002 | 12100011201001010000 | 01100100012001001001 | 00020000101210O1---- | ----1200001001201101 | 21011011000000101010 | 0-01010100 |
| *Tachinus* | 06011010100010100201 | 20-02011111200012000 | 10000010012100001000 | 10111010101211010000 | 00000200001100200011 | 00010-01110110001010 | 0-00100100 |
| *Drusilla* | 010111100---0-100211 | 20-0100-201200010000 | 10000010012103001002 | 00021002201----10000 | 00002100110011200001 | 20010-01110100001010 | 0-21121111 |
| *Glypholoma* | 06011010101010?201 | 0100200-200101010000 | 11001100O?1000001000 | 1002??0-?02112012222 | 00001200001100200011 | 20011021000100000110 | 0-01100100 |
| *Acrolocha* | 05011010102010100201 | 30-10010100001110000 | 00000110012100001000 | 10010000102111O0???? | ????0110100000200001 | 21010-01110110000110 | 0-011000-0 |
| *Oxyporus* | 06011010100010200111 | 30-10011001300010000 | 01100010012100000O0- | --01000002201002222 | 22220201111000200001 | 01010-00100001001010 | 0-10110110 |
| *Stenus* | 0601200-100110100111 | 30-20011113421121000 | 00000011102000001012 | 01020000102111O0???? | ????2211110011200011 | 10011011000001111100 | 0-20122100 |
| *Pseudopsis* | 0411210-100110100212 | 30-20011101201110000 | 00000001102101001112 | 10010000102111002222 | 22222110111000210011 | 20010-00000000001210 | 0-11121101 |
| | O OO O O O O OO OON O OO O O OO O NO O O O O OO O O OOOO OOOO O O OO N N O N O NN O OON | | | | | | |

| | **1111111111** | **1111111111111111111** | **1111111111111111111** | **1111111111111111112** | **2222222222222222222** | **2222222222222222222** | **2222222222222222222** |
|---|---|---|---|---|---|---|---|
| | **3333333334** | **4444444445555555556** | **6666666677777777778** | **8888888899999999990** | **0000000011111111112** | **2222222233333333334** | **4444444455555555556** |
| | **1234567890** | **1234567890123456789O** | **1234567890123456789O** | **1234567890123456789O** | **1234567890123456789O** | **1234567890123456789O** | **1234567890123456789O** |
| *Neopelatops* | 1011320000 | 0010022100000--0-010 | 1210101011000-01-001 | 00101100-12120110001 | 00100000000200011110 | 00000001000-01100000 | 0000-000000010000001 |
| *Necrophilus* | 1001120000 | 0011122100000--0-110 | 1212101011001011001 | 00101100-10120110001 | 10100000000200000110 | 00000001000-01100000 | 0000-00000110-001001 |
| *Thanatophilus* | 1001321000 | 0011022100010--0-012 | 0-0-1010111010111101 | 00102100-10110110001 | 10100000000200111000 | 00000000001000000000 | 0000-010011110000001 |
| *Necrodes* | 1001321110 | 0011022100010--0-011 | 0-0-1100111010111101 | 00102100-10120110001 | 10100000000201111000 | 00000000001000000000 | 0000-000011110000001 |
| *Nicrophorus* | 1001320122 | 0010022100010--0-012 | 0-0-1110111010111101 | 00102100-10110110001 | 10100000001201110000 | 00000000001000000000 | 0000-010012111000001 |
| *Trigonurus* | 1001120100 | 0010021100002100-012 | 1010100111111011001 | 00101100-11120101001 | 00100000000200010001 | 10001100001001100111 | 0000-010012010001001 |
| *Apatetica* | 1001110001 | 0001022100002000-021 | 1212100111101011011 | 00101100-12120101000 | 10000000000200111001 | 10011100001011001220 | 0000-010112010001001 |
| *Nodynus* | 1001120001 | 0001022100002000-022 | 1210110111101011011 | 00102100-12120110001 | 10100000000200111001 | 10001100001011001221 | 0000-010012010001001 |
| *Piestus* | 1001320122 | 0010021100002000-103 | 1212100011111011011 | 00101111111120100001 | 11000000000200000000 | 10001100001001100121 | 0000-010012010000000 |
| *Siagonium* | 1001220122 | 0010022100002000-013 | 1210100011111011001 | 00101011111110100001 | 12000000000200010000 | 11001101001001000221 | 0000-010012010000001 |
| *Hypotelus* | 1001210122 | 0010022100001000-103 | 120-1000111111011011 | 00001101111120100001 | 10000000000200000000 | 00001100001001000221 | 0000-010012010000000 |
| *Eupiestus* | 1001111122 | 0010021000001000-103 | 1011100011111001000 | 00011001011120120001 | 10000000000200000000 | 10001100001101100221 | 0000-010012011000000 |
| *Prognathoides* | 1001320122 | 0010021100001000-103 | 1210100011111011011 | 00101101111120100001 | 10000000000200000000 | 10001100001001110121 | 0000-010012010000001 |
| *Oxypius* | 1001121120 | 0000020000000--0-113 | 0-0-100010-------001 | 00101000-11120100000 | 00000000000000000000 | 10101100001001100111 | 10011010012010010000 |
| *Homalotrichus* | 1001220120 | 0010021100000--0-113 | 1210100011111011011 | 00101101111120110001 | 10000000000200000000 | 10001101001000000221 | 10011010010010000001 |
| *Bledius* | 1001210122 | 0010021100000--0-103 | 0-0-1000111111011011 | 00000100-11110100001 | 10001111110000000000 | 10011101001200002222 | 20011010010011000000 |
| *Ochthephilus* | 1011120120 | 0010021100000--0-113 | 0-0-1000111111011011 | 00000100-11120100001 | 00000202020000000000 | 10011101001200001222 | 20011010010010000000 |
| *Anotylus* | 1011221121 | 0010000000000--0-113 | 110-1000111111011111 | 00002100-10100100001 | 10002020200000000000 | 11011101001200002222 | 20011010-10010000100 |
| *Renardia* | 1001320122 | 0300022110010--0-003 | 0-0-000011110-00-001 | 00000100-0-000110001 | 10000000000200000000 | 10011100001200000000 | 1000-111012010000100 |
| *Eleusis* | 1001310122 | 0300022110000--0-003 | 0-0-000011110-00-001 | 00000100-12100110001 | 10000000000200000001 | 10111100001200000000 | 1000-111012011000100 |
| *Lispinus* | 1001110112 | 0010020100111100-003 | 110-1000111111011001 | 00011100-11010100001 | 10000000000200000001 | 10111100001200000000 | 1000-111012011000100 |
| *Thoracophorus* | 1000111121 | 0000020000002000-113 | 0-0-100010-------001 | 00011101111010100001 | 10000202020100000000 | 10001100011201100000 | 0110-010012010000100 |
| *Paratorchus* | 1000320100 | 0001020100002010-103 | 110-100010-------011 | 00001101011020120001 | 11000202020100000000 | 00101100001001000000 | 0110-110012010000100 |
| *Priochirus* | 1001320112 | 0010021000012011013 | 110-0000111111011001 | 00001000-11020110001 | 11000000000200000001 | 10111100001001100000 | 0110-110012010000000 |
| *Glyptoma* | 1000311121 | 0300020000102100-103 | 0-0-000011110-00-000 | 00011111111000120001 | 00001111110200000000 | 00111100001001100000 | 0110-010012011000001 |
| *Scaphium* | 1000120000 | 0010001000002010-111 | 1210111011011010011 | 11112000-11021100111 | 00100000000201111001 | 00000020101001110222 | 0000-010012010000001 |
| *Scaphidium* | 1000210000 | 0011001000002010-111 | 1210111011011010011 | 11112001011021110111 | 00100000000201111001 | 00000030101001110010 | 0000-010012010000001 |
| *Cyparium* | 1000120000 | 0010001000002010-111 | 1210111011011011011 | 11112001011021100111 | 10100000000201111001 | 00000020101001110221 | 0000-010012010000001 |
| *Scaphisoma* | 1000210000 | 0010001000002010-111 | 110-111011100-00-011 | 1101200100-011100111 | 00100000000201111001 | 00000030101001110111 | 0000-010012010000001 |
| *Tachinus* | 1001120001 | 0011122100010--0-012 | 0-0-1001111110111001 | 00101101011120100001 | 10100000000200111000 | 10001111001200001220 | 0000-010013010000001 |
| *Drusilla* | 1011220102 | 0011002100010--0-003 | 0-0-000010-------001 | 00002000-10020100001 | 00001000000100000000 | 11111101010-00000223 | 00015010011011000000 |
| *Glypholoma* | 1001120100 | 0001022100002000-111 | 1212100111111111011 | 10101101012120101001 | 10100000000200011000 | 00000101001001000110 | 00014000010110001001 |
| *Acrolocha* | 1001120110 | 0000022100000--0-012 | 1212100111111011001 | 00101100-11120101001 | 10100000000200010000 | 10001111001001010111 | 00014000010111000001 |
| *Oxyporus* | 0031000110 | 0010021100000--0-013 | 1210000111111010111010 | 00102110-10110111001 | 00100000000200010000 | 11001101001000001222 | 0000-010012011001001 |
| *Stenus* | 0120310110 | 0100020001000--0-103 | 0-0-0000111110011000 | 00011100-12001021110 | 01000000001000000000 | 10011101011001010110 | 00012000010011010000 |
| *Pseudopsis* | 0011221100 | 0011022100010--0-113 | 0-0-100011110-00-101 | 00100100-12120100001 | 00000000000200000000 | 11001101001000001113 | 00011000110111010001 |
| | N O OO | N O N O NN O | N | O O N | NOOOOOO N | O | O N N N |

**Table 3.** Results of 12 phylogenetic analyses of the Oxyteline Group of Staphylinidae (columns 1 – 12).

**Heading part of table:** "Dataset" row indicates the three datasets used in the analyses (larval morphology, adult morphology, and their combination). "ord./unord." row indicates whether the states in 61 multi-state characters were ordered or unordered. "Successive weighting" row indicates whether successive approximation was used for character weighting. Next three rows indicate tree length, consistency index (CI) and retention index (RI), and the number of the shortest (= most parsimonious) trees (= MPT) obtained.

**Lower main parts of table:** Taxonomic abbreviations in left column: **Oso** – Osoriinae; **Oxy** – Oxytelinae; **Pie** – Piestinae; **Sca** – Scaphidiinae; **OxGr** – Oxyteline Group (Oso + Oxy + Pie + Sca); **Apa** – Apateticinae; **Tri** – Trigonurinae; **Sil** – Silphinae (= Silphidae excluding Nicrophorinae); **SIL** – Silphidae; **STA** – Staphylinidae. **Cell values** in columns 3 and following: presence (+) or absence (–) on the strict consensus tree given before slash, bootstrap value given after slash if > 50%. **Cell color** in columns 3 and following: black – branch highly supported: present on strict consensus tree and bootstrap value ≥ 50%; grey – branch moderately supported: present on strict consensus tree and bootstrap value ≤ 50% OR absent on strict consensus tree but bootstrap value ≥ 50%; white – branch not supported: absent on strict consensus tree and bootstrap ≤ 50%.
Column **RSV** (Relative Support Value) shows how strongly a given clade was supported throughout all 12 analyses; calculated as a ratio of the sum of clade support values obtained in 12 analyses (a sum of 12 horizontal cell scores: 0 for white cells, 1 for grey cells, 2 for black cells) to the possible maximum of 24 (12 analyses × 2); expressed in %. Lowest row **RRV** (Relative Resolution Value) shows how effective each of the 12 analyses was in resolving ingroup relationships as compared to the most consistently supported and fully resolved topology (Fig. 3 based on analysis #9); calculated as a ratio of the sum of support values obtained for each among 11 included clades (a sum of 11 vertical cell scores: 0 for white cells, 1 for grey cells, 2 for black cells) to the possible maximum of 22 (11 clades × 2); expressed in %. Note that in the reference analysis #9 RRV is lower than 100% since some clades in it are not well supported (grey cells).

| | | analysis # | | | | | | | | | | | |
|---|---|---|---|---|---|---|---|---|---|---|---|---|---|
| | RSV | 1 | 2 | 3 | 4 | 5 | 6 | 7 | 8 | 9 | 10 | 11 | 12 |
| dataset | | larvae | larvae | larvae | larvae | adults | adults | adults | adults | comb. | comb. | comb. | comb. |
| ord./unord. | | unord. | unord. | ord. | ord. | unord. | unord. | ord. | ord. | unord. | unord. | ord. | ord. |
| successive weighting | | no | yes | no | yes | no | yes | no | yes | no | yes | no | yes |
| tree length | | 382 | 571 | 442 | 542 | 739 | 795 | 763 | 806 | 1179 | 1250 | 1271 | 1265 |
| CI/RI [%] | | 34/54 | 65/79 | 29/56 | 56/78 | 28/54 | 55/79 | 27/55 | 55/80 | 28/51 | 56/73 | 26/52 | 53/75 |
| # of shortest trees | | 4 | 2 | 640 | 4 | 8 | 1 | 40 | 1 | 4 | 4 | 3 | 1 |
| Clades in single fully and most consistently resolved topology | | | | | | | | | | | | | |
| Oso | 46% | –/– | –/– | –/– | –/– | –/– | +/– | +/– | +/– | +/66 | +/63 | +/63 | +/57 |
| Oxy | 17% | –/– | –/– | –/– | –/– | –/– | –/– | –/– | +/– | +/– | +/– | –/– | +/– |
| Oso + Oxy + Pie | 29% | –/– | –/– | –/– | –/– | –/– | –/– | –/– | +/– | +/55 | +/53 | +/– | +/– |
| Sca | 88% | +/– | +/– | +/52 | +/– | +/100 | +/100 | +/100 | +/100 | +/100 | +/100 | +/100 | +/100 |
| OxGr | 25% | +/– | +/– | +/– | +/– | –/– | –/– | –/– | –/– | +/– | +/– | –/– | –/– |
| Apa | 83% | +/– | –/– | +/62 | –/– | +/96 | +/95 | +/96 | +/97 | +/98 | +/98 | +/95 | +/97 |
| Apa + Tri | 38% | +/54 | +/59 | +/65 | +/– | –/– | –/– | –/– | –/– | +/– | +/– | –/– | –/– |
| SIL | 66% | –/– | –/– | –/– | –/– | +/98 | +/97 | +/98 | +/98 | +/89 | +/91 | +/81 | +/78 |
| STA | 62% | –/– | +/– | –/– | +/– | +/55 | +/57 | –/– | –/51 | +/68 | +/69 | +/65 | +/62 |
| STA ex. (Apa & Tri) | 33% | +/– | +/– | +/57 | +/– | –/– | –/– | –/– | +/– | +/– | +/– | –/– | –/– |
| STA ex. (OxGr & Apa & Tri) | 17% | +/– | –/– | +/– | –/– | –/– | –/– | –/– | –/– | +/– | +/– | –/– | –/– |
| RRV | | 32% | 32% | 45% | 23% | 36% | 41% | 32% | 50% | 77% | 77% | 50% | 55% |
| Alternative clades sought for and undetected | | | | | | | | | | | | | |
| Pie | 0% | –/– | –/– | –/– | –/– | –/– | –/– | –/– | –/– | –/– | –/– | –/– | –/– |
| SIL + Apa | 0% | –/– | –/– | –/– | –/– | –/– | –/– | –/– | –/– | –/– | –/– | –/– | –/– |
| SIL + Apa + Tri | 0% | –/– | –/– | –/– | –/– | –/– | –/– | –/– | –/– | –/– | –/– | –/– | –/– |
| Alternative clades rarely detected and likely artefacts | | | | | | | | | | | | | |
| Sil + Apa + Tri | 17% | +/– | +/– | +/53 | –/– | –/– | –/– | –/– | –/– | –/– | –/– | –/– | –/– |
| STA ex. Sca | 17% | –/– | –/– | –/– | –/– | +/– | +/– | –/– | –/– | –/– | –/– | +/– | +/– |
| SIL + Apa + Sca | 8% | –/– | –/– | –/– | –/– | –/– | –/– | +/– | +/– | –/– | –/– | –/– | –/– |

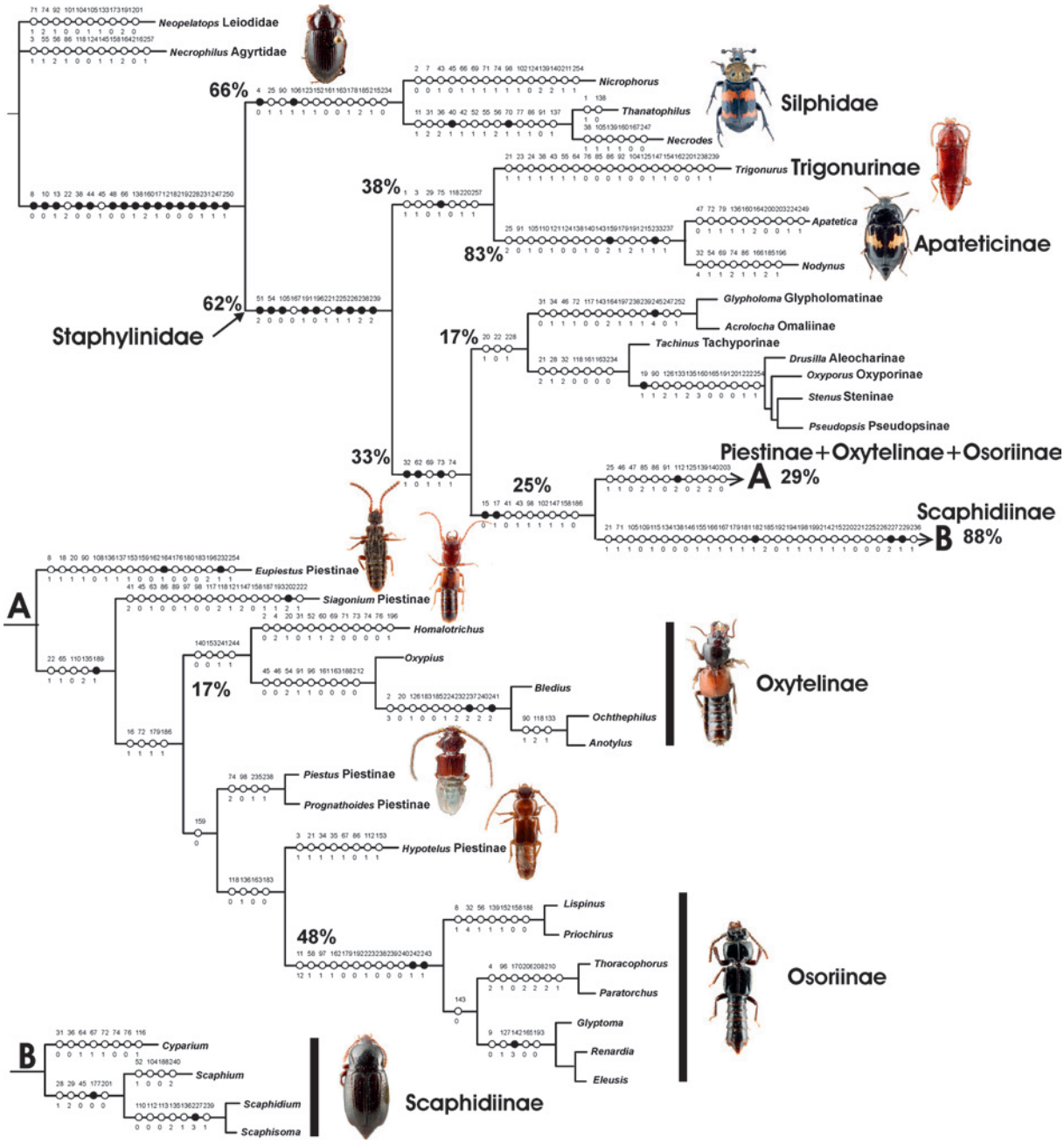


**Fig. 3.** One among four most parsimonious trees from combined analysis of larval and adult morphological data with all characters unordered and equally weighted (analysis #9). Unambiguously optimized evolutionary events common to all four shortest trees are plotted along internodes. Character numbers are above circles; newly acquired character states are below circles. Black circles indicate unique evolutionary events; white circles indicate parallelisms or reversals. Relative Support Value (RVS) as indicated above some clades. Autapomorphies of some terminal branches are removed. Note paraphyly of "Piestinae".

## 4. Discussion

### 4.1. Sister-group relationship and monophyly of Silphidae and Staphylinidae

Although our analysis was originally designed assuming monophyly of the Silphidae + Staphylinidae clade (as supported by many other recent studies, see Introduction), we were able to partially test monophyly of both families (based on the inclusion of an unambiguous out-group taxon from Leiodidae). Both families are indeed found monophyletic. It should be noted that the Relative Support Value for both Silphidae and Staphylinidae was far from absolute (66% and 62%, respectively), which in part might be explained by remarkable morphological variation among the extant species of both clades. The monophyletic family

Staphylinidae was consistently recovered only in the combined data set analyses (#9–12; Table 3), while the partial analyses using either larvae or adults occasionally failed to do so. Even more peculiar is the fact that Silphidae were not recovered as a clade in all four larval analyses (#1–4; Table 3). This might be partly attributed to the extreme morphological differences between the free-living and in some cases actively hunting Silphinae larvae and those of Nicrophorinae developing on buried carcasses and critically dependant on parental care (SIKES 2005).

### 4.2. Basal-most dichotomies of Staphylinidae

The so-called "basal" lineages (= species-poor sister-groups of species-rich clades) always present a peculiar fascination to a biologist. In the context of our study, two species-poor northern hemisphere rove-beetle subfamilies, Apateticinae and Trigonurinae, having 25 and 11 extant species, respectively, were detected as the basal-most off-shoot of the main Staphylinidae clade comprising 57,638 named extant species (Fig. 4). Although these subfamilies are excluded here from the four main staphylinid lineages discussed below, we do not form a new group for them but rather refer them to Staphylinidae *incertae sedis*, pending further studies to confirm or refute this placement.

### 4.3. Interrelationships among the four major Staphylinidae sub-groups

Our results further elucidate the original scheme of the four main rove-beetle radiations originally proposed by LAWRENCE & NEWTON (1982): Omaliinae Group, Tachyporine Group, Oxyteline Group, and Staphylinine Group. During the 30 years since, numerous aberrant beetle "families" have been demonstrated to be phylogenetic offshoots derived from within one of these four major lineages. Thus the former "Dasyceridae", "Micropeplidae" and "Pselaphidae" were placed as subfamilies in the monophyletic Omaliine Group (NEWTON & THAYER 1995), the former "Scaphidiidae" were placed in the Oxyteline Group (first recognized as a staphylinid subfamily by KASULE 1966, placement confirmed in the present study), while the former "Scydmaenidae" were placed in the monophyletic Staphylinine Group (GREBENNIKOV & NEWTON 2009). Monophyly of the Tachyporine Group was assumed (ASHE 2005) and requires confirmation, but has not been contradicted to date, and that of the Oxyteline Group is here corroborated in a slightly restricted sense. The sister-group relations among these four main lineages, however, remain unresolved (Fig. 4), although our results weakly suggest that the Oxyteline Group (*sensu stricto*) might be sister to the rest. Our analysis, however, has not been designed to address this problem and, therefore, we are content to leave it to further scrutiny. At the subfamily level, monophyly has been supported more or less strongly in many recent studies for all of the 32 rove-beetle subfamilies except Piestinae (see 4.5. below) and Tachyporinae and Phloeocharinae (ASHE & NEWTON 1993; not tested in ASHE 2005) (see, e.g., discussions and diagram in THAYER 2005 and NEWTON 2011). The relationships among the numerous rove-beetle subfamilies that form each of the four main groups are at present mainly resolved (see references in Introduction).

### 4.4. Monophyly and composition of the Oxyteline Group

Our analyses consistently identified a monophylum of Scaphidiinae + ("Piestinae" + Osoriinae + Oxytelinae), which we continue to call the Oxyteline Group in a slightly restricted sense (i.e., minus Apateticinae and Trigonurinae, see 4.2. above). As suggested by LAWRENCE & NEWTON (1982), the former "family Scaphidiidae" is here supported to be the sister-group of the remaining three subfamilies. Two unambiguously optimized larval synapomorphies of the clade (Fig. 3) are tentorium having posterior pits in touch (15-0) and corporotentorium attached to the ventral wall of head (17-1).

### 4.5. Monophyly of the individual Oxyteline Group subfamilies

The "subfamily Piestinae" was historically defined by plesiomorphies, such as lacking defensive glands (unlike Oxytelinae), and having paratergites (unlike Osoriinae), as well as adults and larvae being flat and subcortical. Even in the strongly restricted sense used here (excluding the former tribes Apateticini and Trigonurini and various other genera, e.g., as recounted in NEWTON & THAYER 1992), Piestinae has been consistently found as paraphyletic with respect to Osoriinae and Oxytelinae. This suggests that it should be re-evaluated and likely split into two or more monophyletic taxa of subfamily rank. A study by CARON et al. (2012) includes exemplars of all seven remaining genera of "Piestinae" in a phylogenetic analysis, but

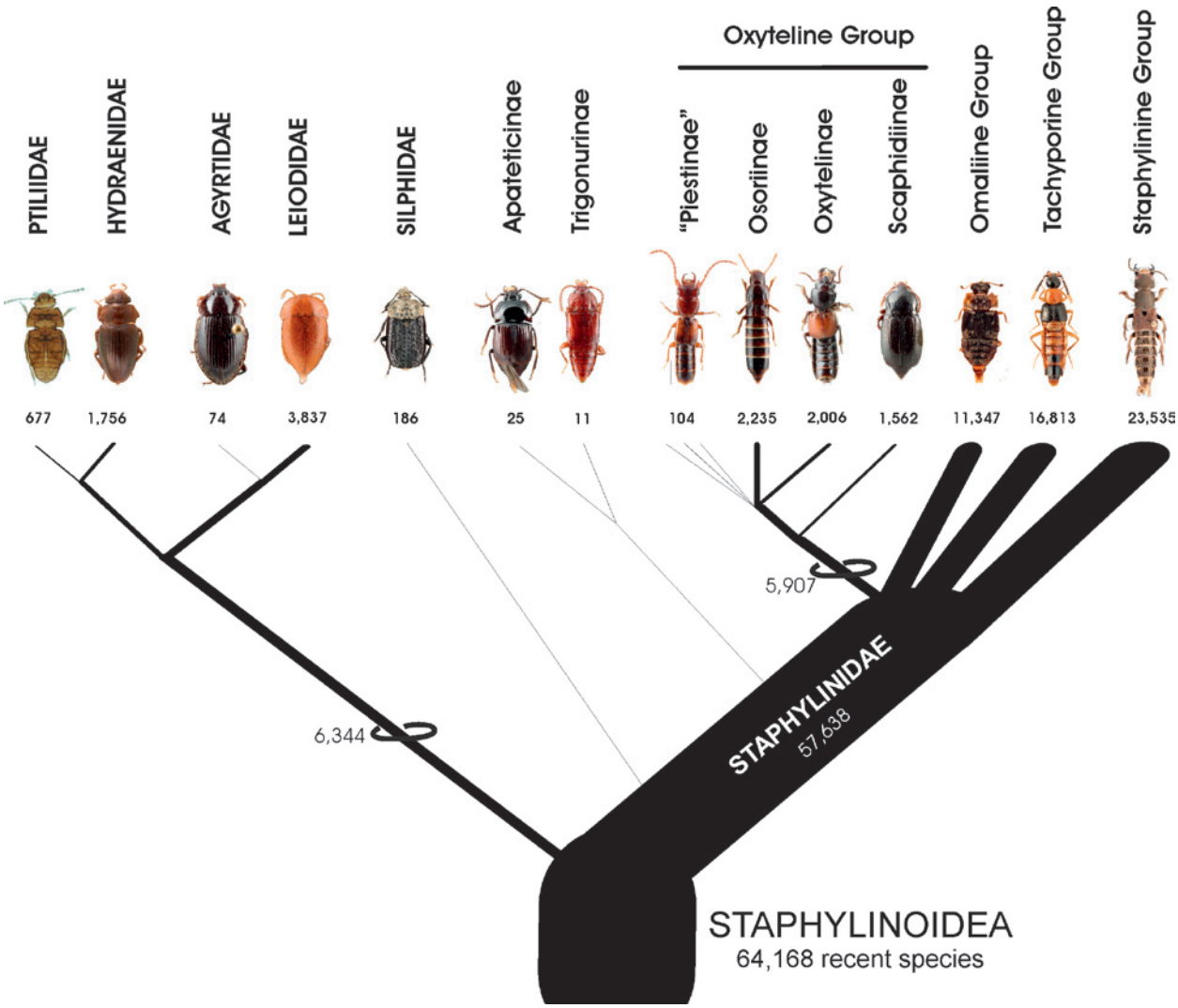


**Fig. 4.** Summary phylogeny of the superfamily Staphylinoidea. Width of branches is proportional to the present-day species richness. Numbers indicate species richness for respective clades as of mid-2011. Note the most contrasting difference in species richness between two sister-families: Silphidae (186 described extant species) and Staphylinidae (57,638 described extant species).

this study was focused on testing the monophyly of one large genus and did not test monophyly of the subfamily as a whole.

The remaining subfamilies of the Oxyteline Group are all supported as monophyletic in our study, and to a large extent the internal relationships among the exemplar genera for each subfamily (not the subject of our analysis, but as suggested in Fig. 3) resemble those in prior phylogenetic studies of two of the subfamilies. Thus, the monophyly of Scaphidiinae and relationships among the four exemplar taxa in our study mirror the conclusions of Leschen & Löbl (1995: fig. 40), and the monophyly of Oxytelinae and relationships among our five exemplar taxa resemble the conclusions of Newton (1982: fig. 41) and Makranczy (2006: fig. 2) if the positions of *Homalotrichus* and *Oxypius* are reversed in our Fig. 3. The monophyly of Osoriinae has not been tested previously but is well supported in our analysis, although the relationships among the seven exemplar taxa in Fig. 3 suggest that the current tribe Thoracophorini (including *Lispinus*, *Thoracophorus* and *Glyptoma* among our exemplars) may not be monophyletic, even though an extensive study of this tribe by Irmler (2010) including these and 21 other genera did find support for such monophyly.

## 4.6. Relative contribution of larval versus adult morphological characters

Like in our earlier work on the Staphylinine Group (Grebennikov & Newton 2009), we employ Relative Resolution Value (RRV, expressed in percentage; horizontal row in Table 3) to compare performance of larval, adult and combined datasets in recovering clades in a way consistent with the reference topology (Fig.

3). The first four analyses employing 82 parsimony-informative larval morphological characters were consistently less powerful (RRV 23–45%, mean 33%, n=4) when compared to the four adult-based analyses with 158 characters (RRV 32–50%, mean 40%, n=4). The four combined dataset analyses (#9 to #12), as would be expected, produced the most meaningful topologies (i.e., consistent with the most consistent and fully resolved one, Fig. 3), with RRV varying between 50% and 77% (mean 65%, n=4). We therefore conclude that in the present analyses, like in our 2009 work, combined analyses were best able to resolve phylogenetic pattern (even though for the lack of an independent reference topology we were obliged to adopt for such one of ours, thus introducing elements of circular logic). In the 2009 Staphylinine Group matrix, however, larval characters were consistently providing better phylogenetic signal, as compared to the adults.

### 4.7. Ancestral conditions of elytral length and feeding mode in Silphidae + Staphylinidae

Elytral length varies greatly in carrion and rove beetles, from completely covering the abdomen as in most other groups of beetles including immediate out-group taxa like Agyrtidae and Leiodidae (very long: some Silphidae-Silphinae, some Staphylinidae including Dasycerinae, Empelinae, Scaphidiinae and most Scydmaeninae), to exposing about half of the abdominal dorsum (moderately long: many Silphidae and several groups of Staphylinidae including Apateticinae, Trigonurinae), to exposing most of the abdominal dorsum (very short: most Staphylinidae) (Fig. 2). Feeding habits also vary greatly, ranging from saprophagous or mycophagous (carrion, dung, humus, rotting cambium and fruits, fresh and decaying fungi, etc., as in most of the immediate out-groups and in Apateticinae, Trigonurinae and Oxyteline Group adults and larvae as well as larvae and some adults of Silphidae) to carnivorous (as in many Silphidae adults, and larvae and adults of most subfamilies of Staphylinidae) (e.g., THAYER 2005).

The evolution of elytral length and feeding mode within rove beetles has been extensively discussed, e.g., by LAWRENCE & NEWTON (1982), NEWTON & THAYER (1995) and GREBENNIKOV & NEWTON (2009). LAWRENCE & NEWTON (1982) hypothesized an ancestral rove beetle (including Silphidae in their concept of the family) as carnivorous and with short elytra, with non-carnivorous feeding and longer elytra being secondary (and not necessarily correlated!) developments within Staphylinidae. They based this on their presumptions about the most likely functional explanations for some morphological characteristics common to all Staphylinidae and apomorphic with respect to immediate outgroups such as Leiodidae and Agyrtidae. Examples for such apomorphies are the very compact wing folding pattern (including a hinge and folding pattern which allows the folded wings to be covered by short elytra) and the loss of a larval mandibular mola or grinding lobe (its presence is correlated in other beetles with microphagous feeding such as saprophagy and mycophagy, and it is almost always lost in carnivorous beetles). Their hypotheses have sometimes been well supported in subsequent studies, e.g., in the case of Scydmaeninae, the most speciose group of rove beetles with long elytra, where GREBENNIKOV & NEWTON (2009) found very strong phylogenetic evidence for the secondary development of long elytra from short elytra in this group. This conclusion was reinforced by the later discovery of Cretaceous fossil Scydmaeninae with much shorter elytra than found in any extant forms (CHATZIMANOLIS et al. 2010).

However, two main results from the present study are not completely in accord with this evolutionary scenario: (1) Apateticinae and Trigonurinae (all saprophagous with moderately long elytra) likely form the sister-group to all remaining Staphylinidae; (2) Silphidae (also with moderately long to long elytra and at least saprophagous larvae) are the sister-group to all Staphylinidae. This indicates that LAWRENCE & NEWTON's (1982) hypothesis about the secondary nature of longer elytra and saprophagy in Silphidae and Staphylinidae can be maintained for more apical staphylinid clades, but it does not apply to the very base of Staphylinidae or to Silphidae. In our analysis (Fig. 3), strongly truncate but not short elytra (apomorphy 160-2) was found as a basal synapomorphy for Staphylinidae + Silphidae, and was retained unchanged in the most basal lineages within both groups, while longer (160-1) and shorter (160-3) elytra are more derived conditions within Staphylinidae and (longer only) Silphidae. Thus the most parsimonious scenario based on our phylogenetic results is that moderately long elytra and saprophagy were present in the ground plans of Silphidae + Staphylinidae, Silphidae, and Staphylinidae, and have both been maintained through the most basal dichotomies within Staphylinidae (from which Apateticinae and Trigonurinae have originated). It follows that saprophagy, which was used in part to justify the original association of subfamilies in the "Oxyteline Group" by LAWRENCE & NEWTON (1982) in contrast to a supposedly carnivorous ancestral staphylinid, is more likely a plesiotypic condition in Staphylinidae, and our conclusion that Apateticinae + Trigonurinae is not closely allied with the remaining subfamilies of the Oxyteline Group is less surprising. Nevertheless, the synapomorphies cited by LAWRENCE & NEWTON (1982) in support of their

"short elytra – larval carnivory" hypothesis of ancestral conditions in Staphylinidae + Silphidae were upheld as synapomorphies for this clade in our analysis (Fig. 3), e.g., loss of a larval mandibular mola (44-0) and presence of a wing hinge (171-1). Evidently it is the functional interpretation of these characters as understood by Lawrence & Newton (1982) and others that requires further study.

### 4.8. Dating the Silphidae and Staphylinidae clades using fossils

Our understanding of the geological record of Silphidae and Staphylinidae is currently undergoing dramatic improvements as the result of many recent fantastic discoveries of Mesozoic fossils, especially of Jurassic and Cretaceous compression fossils from China and Cretaceous amber fossils from Myanmar. Unfortunately, some of the most relevant of these new discoveries are still under study and in the process of being formally described, hence any discussion here must necessarily be very preliminary and subject to change. However, enough is already known (in the case of some new discoveries, known to us) to justify a brief discussion of the minimal ages of these families and to consider whether the known fossils help support or refute our general phylogenetic results.

Although a number of compression fossils as old as Triassic have been attributed to the family Silphidae in its old very broad sense, all of those described fossils older than middle Tertiary (40–50 mya) are misidentified and not even remotely related to Silphidae as now defined (Newton 1997). Recent discoveries of true Silphidae have been made in mid-Jurassic and early Cretaceous sediments in China and are in the process of being described by Chenyang Cai (Nanjing Institute of Geology and Palaeontology, Nanjing, China) and colleagues; most of these have been studied by one of us (AFN) and they are briefly discussed and illustrated in a publicly available online presentation (Thayer et al. 2011). As indicated therein, the mid-Jurassic fossils (165 mya) resemble small modern burying beetles (Nicrophorinae) in appearance and specialized antennal club indicated as a synapomorphy of Silphidae in Fig. 3 (apomorphy 106-1), but are missing some derived features of each of the two modern subfamilies and thus cannot be assigned to either of them; for example, they lack the stridulatory files of abdominal tergum V of modern Nicrophorinae, and possess an epistomal suture, which is absent in all modern Silphinae (apomorphy 91-0 in Fig. 3). Several fossils from the early Cretaceous (125 mya) are similar, but have the stridulatory files on adult abdominal tergum V that are diagnostic of and synapomorphic for modern Nicrophorinae. These Cretaceous silphid fossils can thus be assigned to Nicrophorinae, and they presumably had subsocial habits similar to modern burying beetles that use stridulation to communicate with their larvae (see Sikes 2005). Thus, Silphidae had originated by the mid-Jurassic, and within Silphidae the Nicrophorinae had originated by the early Cretaceous.

The fossil record of Staphylinidae is much more substantial, and dozens of Jurassic and Cretaceous fossils have been described, with many more under study. The oldest fossils attributed to Staphylinidae are from late Triassic deposits of Virginia (ca. 225 mya) and have been formally described as *Leehermania prorova* and discussed in the context of a review of all Mesozoic rove beetle fossils by Chatzimanolis et al. (2012). Those authors noted that *Leehermania* has the general characteristics of Staphylinidae including relatively short elytra and slender unclubbed antennae (apomorphy 105-0 in our Fig. 3). They considered it closest to members of the Tachyporine Group because of its having a tapered abdomen, but placed the genus as Staphylinidae incertae sedis. Based primarily on the review of *Leehermania* and other Mesozoic staphylinid fossils by Chatzimanolis et al. (2012), and augmented by Solodovnikov et al. (2012), the following comments can be made (per our interpretation, not necessarily the conclusions of Chatzimanolis et al. 2012):

**(1)** *Leehermania prorova* somewhat resembles modern Trigonurinae (Fig. 1F) and some Tachyporinae in shape, but not in many structural details (e.g., it lacks abdominal paratergites, unlike those modern groups, but there is no clear view of the ventral side, so many important characters are not visible), and apparently is not assignable to Trigonurinae, Tachyporinae or any other modern subfamily of Staphylinidae. We consider the assignment of *Leehermania* to Staphylinidae to be uncertain, since some possible alternative family assignments were not considered in detail or at all by Chatzimanolis et al. (2012). In particular, *Leehermania* resembles Hydroscaphidae (suborder Myxophaga) in many characters including small size, overall body shape, short elytra, lack of abdominal paratergites, very short antennae and legs, and weak antennal club tapered at both ends, as evident when it is compared to the recently described early Cretaceous fossil *Hydroscapha? jeholensis* Cai et al. (2012), or to modern hydroscaphids; the latter authors even noted the superficial similarity of the hydroscaphid fossil to tachyporine Staphylinidae. Definitive placement of *Leehermania* will require further study and, ideally, discovery of additional fossils with a well-preserved ventral view.

**(2)** The Jurassic fossils (middle to late Jurassic), many of which are well-preserved with dorsum and

venter clearly visible, include 16 extinct genera (22 extinct species), of which 12 genera have been plausibly assigned to the 6 modern subfamilies Olisthaerinae (*Anicula* Ryvkin), Omaliinae (*Archodromus* Tikhomirova, *Eophyllodrepa* Ryvkin, *Globoides* Tikhomirova, *Morsum* Ryvkin, *Porrhodromus* Tikhomirova), Oxytelinae (*Mesoxytelus* Tikhomirova), "Piestinae" in its former broad concept (*Abolescus* Tikhomirova, more plausibly placed in Trigonurinae), Scaphidiinae (*Scaphidiopsis* Handlirsch) and Tachyporinae (*Abscondus* Tikhomirova, *Mesotachinus* Tikhomirova, *Tachyporoides* Tikhomirova), and 4 genera are considered Staphylinidae *incertae sedis*.

**(3)** The Cretaceous fossils, likewise often well-preserved with dorsum and venter visible in detail, include 33 extinct genera (59 extinct species) and members of 6 extant genera (7 extinct species), of which 28 extinct genera and the 6 extant genera have been plausibly assigned to the 12 modern subfamilies Euaesthetinae (2 extant genera), Omaliinae (3 extinct genera), Oxyporinae (1 extant genus), Oxytelinae (4 extinct and one extant genus), Paederinae (1 extinct genus), Phloeocharinae (1 extant genus), Scydmaeninae (5 extinct genera), Solieriinae (1 extinct genus), Staphylininae (6 extinct genera), Steninae (1 extant genus), Tachyporinae (6 extinct genera) and Trigonurinae (2 extinct genera), and 5 genera are considered Staphylinidae *incertae sedis*.

Undescribed materials from the mid-Jurassic through early Cretaceous of China that are under study and partially seen by AFN will greatly expand the known diversity of staphylinids from this period. This includes numerous examples of Trigonurinae, possible Apateticinae, and Glypholomatinae among others.

The staphylinid fossils referred to above thus document that the family Staphylinidae had originated by the late Triassic (if *Leehermania* is accepted as Staphylinidae) or in any case by mid-Jurassic; had diversified into at least 6 modern subfamilies by the late Jurassic (including members of the Omaliine, Oxyteline and Tachyporine Groups as well as Trigonurinae among the informal "basal" group identified in our study); and had further diversified in the Cretaceous into at least 14 modern subfamilies (including members of all subfamily groups).

To conclude, the available and growing fossil evidence allows us to date the origin of the Silphidae + Staphylinidae clade, as well as the family Staphylinidae, to possibly at or before the late Triassic, or definitely at latest to the mid-Jurassic; the separation of Silphidae and Staphylinidae to no later than mid-Jurassic; and the origin of most if not all of the major staphylinid lineages (groups) and many of its subfamilies to some time during the Jurassic. These conclusions are generally consistent with our phylogenetic results as summarized in Fig. 4, and date the divergence of the main staphylinid subfamily groups shown there to the Jurassic, with the possible exception of the Staphylinine Group which is not confirmed as present until earliest Cretaceous.

## 5. Acknowledgements

Accumulation of the studied larval and adult Staphylinoidea beetles was assisted by the collecting efforts of numerous people, most notably Margaret Thayer (Chicago, USA), and by support from the U.S. National Science Foundation PEET (Partnerships for Enhancing Expertise in Taxonomy) Grant No. 0118749 to the Field Museum of Natural History (Principal Investigator M. Thayer); field work was also supported by the National Geographic Society and the Marshall Field Fund of the Field Museum of Natural History. We also thank M. Thayer for the use of the photographs in Figs. 9–11, taken as part of the Staphyliniformia TWiG subcontract to M. Thayer/FMNH in the U.S. NSF-funded project, AToL: Assembling the Beetle Tree of Life (Principal Investigators B. Farrell, D. Maddison & M. Whiting, awards EF-0531768, EF-0531754, EF-0531665). Karen McLachlan Hamilton (Ottawa, Canada) reviewed this paper prior to submission, and Margaret Thayer provided useful comments to parts of it. Jan Růžička (Prague, Czech Republic) reviewed the manuscript. Artem Zaitsev (Moscow, Russia) identified larvae of *Nodynus leucofasciatus*, prepared their illustrations (Fig. 6) and permitted their use. Results reported in this paper were presented in 2011 at the 5th Dresden Meeting on Insect Phylogeny, for which VVG's participation was supported by the Alexander von Humboldt Foundation (www.avh.de). We also thank Chenyang Cai (Nanjing, China) and Stylianos Chatzimanolis (Chattanooga, USA) for comments about fossils and access to fossil materials and unpublished work in progress. Finally, we thank the editor, Klaus Klass, for much useful input that significantly improved the manuscript.

## 6. References

ASHE J.S. 2005. Phylogeny of the tachyporine group subfamilies and "basal" lineages of the Aleocharinae (Coleoptera: Staphylinidae) based on larval and adult characteristics. – Systematic Entomology **30**: 3–37.

ASHE J.S., NEWTON A.F. 1993. Larvae of *Trichophya* and phylogeny of the tachyporine group of subfamilies (Coleoptera: Staphylinidae) with a review, new species and characterization of the Trichophyinae. – Systematic Entomology **18**: 267–286.

BEUTEL R.G., LESCHEN R.A.B. 2005. Phylogenetic analysis of Staphyliniformia (Coleoptera) based on characters of larvae and adults. – Systematic Entomology **30**: 510–548.

Beutel R.G., Molenda R. 1997. Comparative morphology of selected larvae of Staphylinoidea (Coleoptera, Polyphaga) with phylogenetic implications. – Zoologischer Anzeiger **236**: 37–67.

Cai Chenyang, Short A.E.Z., Huang Diying 2012. The first skiff beetle (Coleoptera: Myxophaga: Hydroscaphidae) from Early Cretaceous Jehol biota. – Journal of Paleontology **86**(1): 1136–1139.

Caron E., Ribeiro-Costa C.S., Newton A.F. 2012. Cladistic analysis and revision of *Piestus* Gravenhorst, with remarks on related genera (Coleoptera: Staphylinidae: Piestinae). – Invertebrate Systematics **25**(6): 490–585.

Caterino M.S., Hunt T., Vogler A.P. 2005. On the constitution and phylogeny of Staphyliniformia (Insecta: Coleoptera). – Molecular Phylogenetics and Evolution **34**(3): 655–672.

Chatzimanolis S., Engel M.S., Newton A.F., Grimaldi D.A. 2010. New ant-like stone beetles in mid-Cretaceous amber from Myanmar (Coleoptera: Staphylinidae: Scydmaeninae). – Cretaceous Research **31**(1): 77–84.

Chatzimanolis S., Grimaldi D.A., Engel M.S., Fraser N.C. 2012. *Leehermania prorova*, the earliest staphyliniform beetle, from the Late Triassic of Virginia (Coleoptera: Staphylinidae). – American Museum Novitates **3761**: 1–28.

Dobler S., Müller J.K. 2000. Resolving phylogeny at the family level by mitochondrial cytochrome oxidase sequences: phylogeny of carrion beetles (Coleoptera, Silphidae). – Molecular Phylogenetics and Evolution **15**(3): 390–402.

Farris J.S. 1969. A successive approximation approach to character weighting. – Systematic Zoology **18**: 374–385.

Farris J.S. 1988. Hennig86. – Published by the author, Port Jefferson Station, New York.

Goloboff P. 1999. NONA, Version 2. – Published by the author, Tucumán, Argentina.

Grebennikov V.V., Newton A.F. 2009. Good-bye Scydmaenidae, or why the ant-like stone beetles should become megadiverse Staphylinidae *sensu latissimo* (Coleoptera). – European Journal of Entomology **106**: 275–301.

Hansen M. 1997. Phylogeny and classification of the staphyliniform beetle families (Coleoptera). – Biologiske Skrifter, Det Kongelige Danske Videnskabernes Selskab **48**: 1–339.

Herman L.H. 1970. Phylogeny and reclassification of the genera of the rove-beetle subfamily Oxytelinae of the world (Coleoptera, Staphylinidae). – Bulletin of the American Museum of Natural History **142**: 343–454.

Herman L.H. 1975. Revision and phylogeny of the monogeneric subfamily Pseudopsinae for the world (Staphylinidae, Coleoptera). – Bulletin of the American Museum of Natural History **155**: 243–317.

Hunt T., Bergsten J., Levkanicova Z., Papadopoulou A., St. John O., Wild R., Hammond P.M., Ahrens D., Balke M., Caterino M.S., Gómez-Zurita J., Ribera I., Barraclough T.G., Bocakova M., Bocak L., Vogler A.P. 2007. A comprehensive phylogeny of beetles reveals the evolutionary origins of a superradiation. – Science **318**: 1913–1916; supporting online material, 31 pp., 2 unpaged tables.

Irmler U. 2010. A new genus of Osoriinae in the Neotropical region with a cladistic analysis of the tribe Thoracophorini (Insecta: Coleoptera: Staphylinidae). – Arthropod Systematics & Phylogeny **68**(2): 229–237.

Kasule F.K. 1966. The subfamilies of the larvae of Staphylinidae (Coleoptera) with keys to the larvae of the British genera of Steninae and Proteininae. – Transactions of the Royal Entomological Society of London **118**: 261–283.

Lawrence J.F., Newton A.F. 1982. Evolution and classification of beetles. – Annual Review of Ecology and Systematics **13**: 261–290.

Lawrence J.F., Ślipiński A., Seago A.E., Thayer M.K., Newton A.F., Marvaldi A.E. 2011. Phylogeny of the Coleoptera based on morphological characters of adults and larvae. – Annales Zoologici **61**(1): 1–217.

Leschen R.A.B., Löbl I. 1995. Phylogeny of Scaphidiinae with redefinition of tribal and generic limits (Coleoptera: Staphylinidae). – Revue Suisse de Zoologie **102**: 425–474.

Madge R.B. 1980. A catalogue of type-species in the family Silphidae (Coleoptera). – Entomologica Scandinavica **11**(3): 353–362.

Makranczy G. 2006. Systematics and phylogenetic relationships of the genera in the *Carpelimus* group (Coleoptera: Staphylinidae: Oxytelinae). – Annales Historico-Naturales Musei Nationalis Hungarici **98**: 29–120.

Naomi S.-I. 1988. Comparative morphology of the Staphylinidae and the allied groups (Coleoptera, Staphylinoidea). VI. Mesothorax and metathorax. – Kontyû **56**: 727–738.

Newton A.F. 1982. A new genus and species of Oxytelinae from Australia, with a description of its larva, systematic position, and phylogenetic relationships (Coleoptera: Staphylinidae). – American Museum Novitates **2744**: 1–24.

Newton A.F. 1997. Review of Agyrtidae (Coleoptera), with a new genus and species from New Zealand. – Annales Zoologici **47**: 111–156.

Newton A.F. 2007. Documenting biodiversity: how well are we doing in Staphyliniformia (Coleoptera)? Entomological Society of America poster presentation D0471. Available (ESA members only) at <http://esa.confex.com/esa/2007/techprogram/paper_32168.htm>.

Newton A.F. 2011. Phylogenie und Systematik. Pp. 1–4 in: Assing V., Schülke M. (eds.), Die Käfer Mitteleuropas, Band 4, Staphylinidae (exklusive Aleocharinae, Pselaphinae und Scydmaeninae), 2. Auflage. – Spektrum Akademischer Verlag, Heidelberg.

Newton A.F., Thayer M.K. 1992. Current classification and family-group names in Staphyliniformia (Coleoptera). – Fieldiana: Zoology (N.S.) **67**: 1–92.

Newton A.F., Thayer M.K. 1995. Protopselaphinae new subfamily for *Protopselaphus* new genus from Malaysia, with a phylogenetic analysis and review of the Omaliine Group of Staphylinidae including Pselaphidae (Coleoptera). Pp. 219–320 in: Pakaluk J., Ślipiński S.A. (eds.), Biology, Phylogeny, and Classification of Coleoptera: Papers Celebrating the 80th Birthday of Roy A. Crowson. – Muzeum i Instytut Zoologii PAN, Warszawa.

NEWTON A.F., THAYER M.K. 2005. Catalog of higher taxa, genera and subgenera of Staphyliniformia [online]. Chicago: Field Museum of Natural History [last updated 27 August 2005]. Available at <http://archive.fieldmuseum.org/peet_staph/db_1a.html>.

NIXON K.C. 2002. WinClada, Version 1.0000. – Published by the author, Ithaca, NY, USA.

SIKES D.S. 2005. Silphidae Latreille, 1807. Pp. 288–296 in: BEUTEL R.G., LESCHEN R.A.B. (eds.), Coleoptera, Beetles, Vol. 1: Morphology and Systematics (Archostemata, Adephaga, Myxophaga, Polyphaga partim). Handbook of Zoology, Vol. IV: Arthropoda: Insecta, Part 38. – Walter de Gruyter, Berlin & New York.

SOLODOVNIKOV A., YUE YANLI, TARASOV S., REN DONG 2012. Extinct and extant rove beetles meet in the matrix: Early Cretaceous fossils shed light on the evolution of a hyperdiverse insect lineage (Coleoptera: Staphylinidae: Staphylininae) – Cladistics: early view, 44 pp., DOI 10.1111/j.1096-0031.2012.00433.x.

THAYER M.K. 2000. *Glypholoma* larvae at last: phylogenetic implications for basal Staphylinidae? (Coleoptera: Staphylinidae: Glypholomatinae). – Invertebrate Taxonomy **14**: 741–754.

THAYER M.K. 2005. Staphylinidae Latreille, 1802. Pp. 296–344 in: BEUTEL R.G., LESCHEN R.A.B. (eds.), Coleoptera, Beetles, Vol. 1: Morphology and Systematics (Archostemata, Adephaga, Myxophaga, Polyphaga partim). Handbook of Zoology, Vol. IV: Arthropoda: Insecta, Part 38. – Walter de Gruyter, Berlin & New York.

THAYER M., CAI CHENYANG, PARDO F. 2011. Fossil carrion feeders. Field Museum of Natural History, Chicago. Video only, online at <http://fieldmuseum.org/explore/multimedia/video-fossil-carrion-feeders>; online and downloadable as mp4 file from Vimeo: <http://www.vimeo.com/27216645> (both accessed 5 December 2012).

# Appendix 1

List of 260 morphological characters used in the analysis. When critical, we indicate in square parentheses the direction from which we examined the structure.

## Larvae: body and head

**1.** Apically frayed setae anywhere on body [dorsal view]: absent = 0; present = 1 (Fig. 7H).

**2.** Stemmata, number [lateral view]: nil = 0; one = 1; two = 2; three = 3; four = 4; five = 5; six = 6 (Figs. 5D, 7A).

**3.** Markedly developed toothed microsculpture on body sclerites, urogomphi and legs (at least in the older instars, as in *Necrophilus*): absent = 0; present = 1 (Fig. 5G,I).

**4.** Head, width [dorsal view]: ≤0.8× width of prothorax = 0; 0.9–1.0× width of prothorax = 1; ≥1.1× width of prothorax = 2.

**5.** Extension of coronal suture from its starting point on posterior margin of head capsule, compared to total length of head capsule [dorsal view]: <0.2× = 0; 0.3–0.5× = 1 (Fig. 8A); >0.5× = 2.

**6.** Dorsal ecdysial lines [dorsal view]: Y-shaped, maximal width between apices = 0 (Fig. 5F); lyriform, maximal width posteriorly of apices = 1 (Fig. 8A).

**7.** Hypostomal ridge [ventral view]: absent = 0; present = 1 (Fig. 5M).

**8.** Posterior extension of hypostomal ridge [ventral view]: not reaching posterior tentorial pits = 0 (Fig. 8B); reaching posterior tentorial pits = 1.

**9.** Posterior tentorial arms [ventral view]: absent = 0; present = 1.

**10.** Posterior extension of posterior tentorial arms [ventral view]: joining tentorial bridge = 0; joining occipital rim = 1.

**11.** Posterior tentorial arms, anterior attachment [ventral view]: to the rest of tentorium = 0; to occipital rim and connected with the rest of tentorium = 1; to occipital rim and not connected with the rest of tentorium = 2.

**12.** Posterior tentorial arms, width [ventral view]: <20× as long as wide = 0; >30× as long as wide = 1.

**13.** Tentorial bridge [ventral view]: absent = 0; present, even if extremely thin and thread-like = 1.

**14.** Tentorial bridge, anterior attachment [ventral view]: posterior tentorial arms = 0; occipital rim = 1.

**15.** Transverse distance between posterior pits [ventral view]: pits touching each other or forming a single pit = 0; not touching and distance not

greater than width of widest maxillary palpomere = 1 (Fig. 5M); distance greater than in state 1, but smaller than width of submentum = 2; distance greater than width of submentum = 3.

**16.** Posterior tentorial pits, shape and number [ventral view]: two curved pits = 0; single transverse straight pit (Fig. 8B) = 1.

**17.** Corporotentorium, location and shape [ventral view]: deeply inside head capsule and connected to ventral head wall by ventral tentorial arms = 0 (Fig. 5N); attached to ventral wall of head capsule, even if reduced is size = 1.

**18.** Ventro-medial edges of epicranial plates, length [ventral view]: not longer than width of maxillary palpomere (Fig. 8B) = 0; longer than state 0 and shorter than length of prementum = 1; subequal to or longer than length of prementum = 2 (Fig. 5M).

**19.** Gula [ventral view]: absent = 0 (Fig. 19B); present = 1.

**20.** Sclerotized strip separating dorsal mandibular articulation from antennal attachment [dorsal view]: very narrow and almost invisible = 0 (Fig. 8A); wider, half width of antennomere 1 = 1; subequal in width to antennomere 1 = 2.

**21.** Dorsal mandibular articulation, location relative to mid-point of antennal articulating membrane [dorsal view]: antero-mesad = 0; anterad = 1; antero-laterad = 2 (Fig. 8A); laterad = 3.

**22.** Internal transverse ridge formed by anterior tentorial arm attachment [dorsal view]: absent = 0; present, short = 1; present, long = 2 (Fig. 5F).

**23.** Internal transverse ridge between anterior tentorial arm attachment and dorsal mandibular condyle, shape [dorsal view]: straight = 0 (Fig. 5F); curved = 1.

**24.** Labrum and clypeus [dorsal view]: separated by distinct suture visible at full length = 0 (Fig. 5F); partly fused with only lateral parts of the suture visible = 1; fused to clypeus without traces of the suture = 2.

**25.** Number of lateral sclerites on each side of labrum near its articulation/fusion to clypeus [dorsal view]: nil = 0; one = 1; two = 2 (Fig. 5F).

**26.** Labrum/nasale, symmetry [dorsal view]: symmetrical = 0; asymmetrical = 1 [uninformative and deactivated].

**27.** Labrum/nasale, anterior edge, presence of teeth [dorsal view]: absent, edge even, not toothed or serrate = 0 (Fig. 8A); present, edge toothed or serrate = 1.

**28.** Labrum/nasale, anterior edge, heterogeneity among teeth [dorsal view]: teeth uneven, longest teeth $>3\times$ as long as the shortest = 0; evenly serrate, longest teeth $<2\times$ as long as the shortest = 1.

**29.** Labrum/nasale, anterior edge, main outline at middle (excluding teeth or serration) [dorsal view]: convex = 0; straight = 1; concave = 2.

**30.** Median tooth on labrum/nasale [dorsal view]: absent or undistinguishable in even serration = 0; present and clearly distinguishable = 1.

**31.** Antennae, length compared to length of head capsule [dorsal view]: $<0.5\times$ = 0; $0.5–0.8\times$ = 1; $0.9–1.1\times$ = 2 (Fig. 7A); $>1.2\times$ = 3 (Fig. 5E).

**32.** Antennomere 1, shape [dorsal view]: wider than long = 0; $1.0–1.5\times$ as long as wide = 1; $1.5–2.0\times$ as long as wide = 2; $2.0–3.0\times$ as long as wide = 3; $>3.0\times$ as long as wide = 4.

**33.** Main sensory antennal appendage on penultimate antennomere, its position with respect to articulation of apical antennomere [dorsal view]: anterior/mesal = 0 (Fig. 5G); ventral = 1; dorsal = 2.

**34.** Main sensory antennal appendage, shape [dorsal view]: bulbous or conical, with convex sides = 0 (Fig. 5G); parallel-sided along much of its length = 1.

**35.** Main sensory antennal appendage, length compared to maximal width of penultimate antennomere [dorsal view]: shorter = 0 (Fig. 5G); as long as, or longer than = 1.

**36.** Third (ultimate or apical) antennomere, shape [dorsal view]: absent, deformed, or shortened, length to width ratio 1.0 and less = 0; of regular shape or slightly shortened, length to width ratio 1.5–3.0 (Fig. 8A) = 1; markedly elongate, length to width ratio more than 3.0 = 2.

**37.** First (basal) antennomere, sclerotization [dorsal view]: complete, not constricted or transversely interrupted by membrane = 0 (Fig. 8B); constricted by a sclerotized ring into two pseudosegments = 1; interrupted by a membranous ring into two pseudosegments = 2.

**38.** Seta or setae on first (basal) antennomere [dorsal view]: absent = 0; present = 1 (Fig. 7A).

**39.** Setae on second (penultimate) antennomere, number [dorsal view]: 3 = 0; >3 = 1 (Fig. 7A).

**40.** Long setae in apical half of third (ultimate or apical) antennomere (excluding non-articulated seta-like sensory structures) [dorsal view]: 3 = 0; >3 = 1.

**41.** Mandible, angle of medial outline between widened basal and narrowed apical parts [dorsal view]: absent = 0; present, smooth or forming obtuse angle = 1 (Fig. 5K); present, sharp, forming right angle = 2 (Fig. 7C).

**42.** Mandibles, maximal number of subapical teeth in apical quarter (excluding serration and the main mandibular apex) [dorsal view]: nil, subapical teeth absent = 0; one = 1 (Fig. 5K); two = 2; three = 3.

**43.** Mandibular apices, shape [dorsal view]: acutely pointed = 0 (Fig. 5K); bifid, multifid or variously shaped, not acute = 1 (Fig. 7C).
**44.** Mandibular mola [dorsal view]: absent = 0; present = 1.
**45.** Mandibles, width at base compared to width at middle [dorsal view]: 1–1.5 = 0; 1.7–3 = 1 (Fig. 7C); 5.0–7.0 = 2.
**46.** Mandibles, symmetry [dorsal view]: symmetrical or almost symmetrical = 0; slightly asymmetrical = 1; markedly asymmetrical = 2.
**47.** Mandibles, mesal serration [dorsal view]: absent = 0; present, even if not along entire length = 1.
**48.** Mandibles, shape [dorsal view]: relatively straight or slightly curved, apices when open directed anteriorly = 0; markedly curved, apices when open directed almost mesally = 1.
**49.** Mandibles, mesal profile [dorsal view]: various, but not not sickle-shaped = 0; sickle-shaped = 1.
**50.** Cardo, transverse ridge on its sclerotized part [ventral view]: absent = 0; present = 1 (Fig. 5M).
**51.** Galea and lacinia (or mala, if fused) [ventral view]: divided in distal 1/3 to 1/4 and fully fused in proximal part = 0; divided in distal 1/10 and fully fused in proximal part = 1; completely fused along entire length forming undivided mala = 2 (Fig. 5L).
**52.** Galea and lacinia (or mala, if fused), shape [ventral view]: widest at base = 0; widest distad of base = 1.
**53.** First (basal) maxillary palpomere (the one apicad of maxillary palpifer), setae [ventral view]: absent = 0; present = 1 [uninformative and deactivated].
**54.** First (basal) maxillary palpomere (the one apicad of maxillary palpifer), length compared to length of second maxillary palpomere: ≤0.8 × = 0; subequal = 1; 1.1–1.9 × = 2; ≥2.0 × = 3.
**55.** Second (penultimate) maxillary palpomere, number of setae [ventral or dorsal view]: 2 = 0; >2 = 1.
**56.** Third (apical) maxillary palpomere, number of setae exceeding in length the width of palpomere [ventral or dorsal view]: nil = 0; one = 1; more than one = 2.
**57.** Ligula [ventral view]: absent = 0; present = 1 (Fig. 8B).
**58.** Mentum and submentum, ventral sclerotization [ventral view]: indistinct, if distinct, then transversely interrupted by membrane = 0 (Fig. 5O); distinct and fused forming single plate = 1.
**59.** Submentum laterally, whether free from head capsule [ventral view]: free = 0 (Fig. 5O); fused = 1.
**60.** Ligula, proportions [ventral view]: longer than wide = 0; about as long as wide = 1; wider than long = 2 (Fig. 8B).
**61.** Ligula, width at apex compared to width of basal labial palpomere [ventral view]: ≥1.5 × = 0 (Figs. 5O, 8B); ≤1 × = 1.
**62.** Ligula, shape at apex [ventral view]: pointed, rounded or straight, not broadly bilobed at apex = 0 (Fig. 8B); broadly bilobed or tetralobed at apex (by a notch at middle) = 1 (Fig. 5O).
**63.** Prementum, ventral sclerite [ventral view]: indistinct or, if distinct, then entire = 0 (Fig. 8B); longitudinally subdivided along midline by membrane = 1.
**64.** Labial palp, width of basal separation compared to palp width [ventral view]: 0.9–1.3 × = 1; >1.5 × = 2 (Figs. 5O, 8B).

## Larvae: thorax

**65.** Cervicosternum (= eusternum) [ventral view]: subdivided by membrane, consisting of several sclerites or, apparently, membranose = 0 (Fig. 5E); entire, consisting of a single sclerite = 1.
**66.** Longest seta on legs, location [lateral view]: on trochanter = 0 (Fig. 7G); no clearly defined longest seta = 1; on femur = 2.
**67.** Tibiotarsus, shape [dorsal view]: evenly sided = 0 (Fig. 7G); abruptly widened at middle = 1.
**68.** Tibiotarsus, number of setae: <10 = 0; 10–20 = 1; >20 = 2 (Fig. 7G).

## Larvae: abdomen

**69.** Abdomen, shape [dorsal view]: evenly narrowing posterad = 0; parallel-sided most of its length = 1; widening posterad to about 1.2 of thoracic width = 2.
**70.** Lateral tergal lobes extending laterally and overhanging body sides [dorsal view]: absent = 0; present = 1.
**71.** Pygidium (segment X), shape: distinctly wider than long = 0; about as wide as long = 1; distinctly longer than wide = 2 (Fig. 5J).
**72.** Urogomphi, number of segments [dorsal view]: one = 1; two = 2 (Fig. 7I).
**73.** Urogomphi, long apical seta (at least 25% of urogomphal length) [dorsal view]: absent = 0 (Fig. 7I); present = 1.
**74.** Urogomphi, length compared to length of tergum VIII [dorsal view]: ≤1 × = 0; 1–1.5 × = 1; 2 × = 2; ≥3 × = 3 (Fig. 7I).
**75.** Urogomphi, ring-shaped microsculpture [dorsal view]: absent = 0; present = 1 (Fig. 7I).

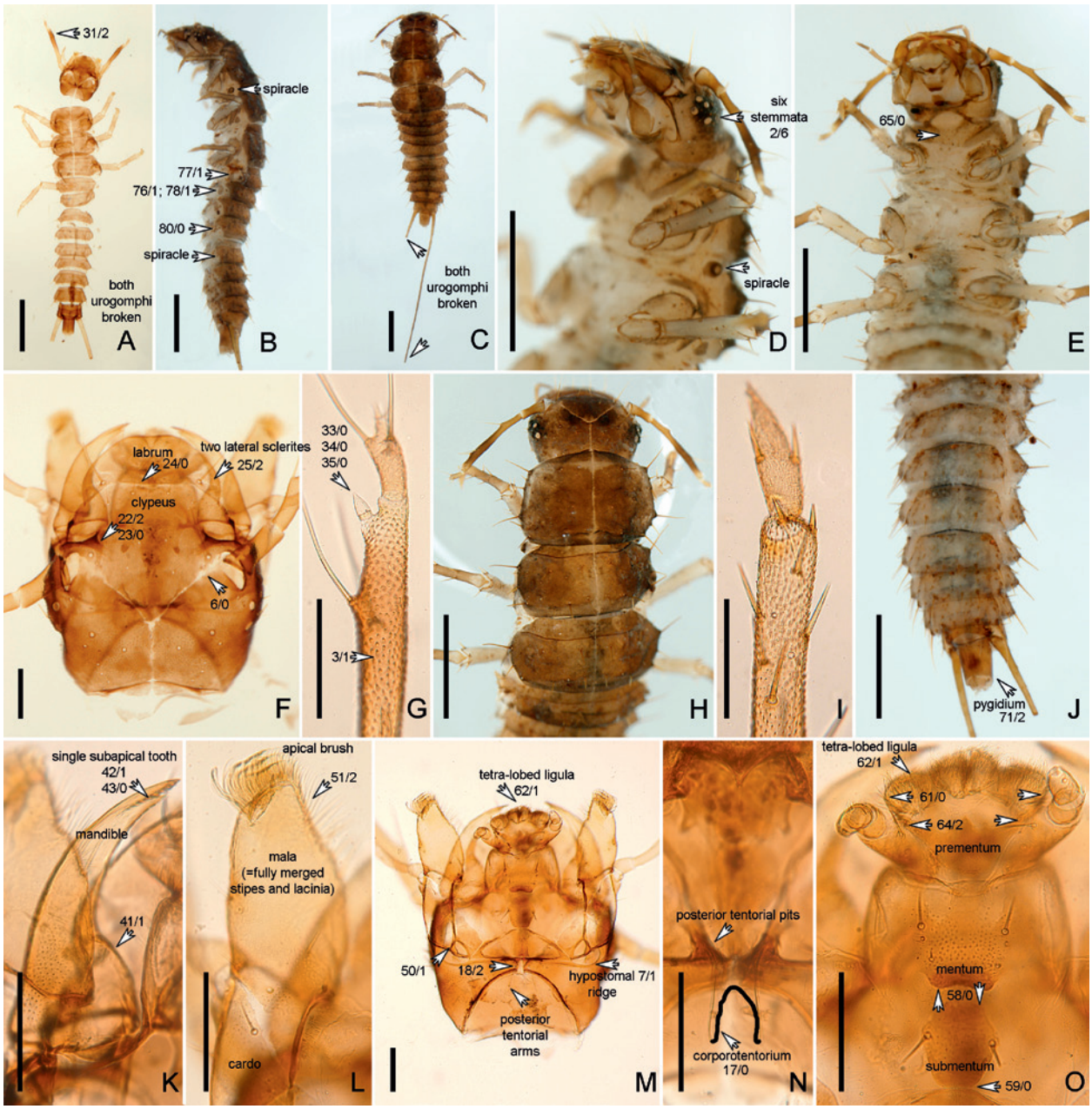


**Fig. 5.** *Apatetica* sp. (Apateticinae) larva; dorsal (A, C, F–H, K), lateral (B, D) and ventral (E, I–O); younger (?second) (A) and older (?third) (B–O) instars; **A**–**C**: habitus; **D**, **E**, **H**: anterior body; **F**, **M**: head; **G**: apex of right antenna; **I**: right middle leg; **J**: posterior body; **K**: left mandible; **L**: right maxillary mala; **N**: venter of head capsule showing posterior tentorial pits, posterior tentorial arms connected by thread-like corporotentorium (blackened to be visible); **O**: mentum and labrum.

**76.** Abdominal sclerites, sclerotization [dorsal or ventral view]: not distinguishable from surrounding membrane = 0; clearly distinguishable from surrounding membrane = 1 (Fig. 5B).

**77.** Abdominal segment 1, laterotergites [lateral view]: absent = 0; present, one = 1 (Fig. 5B); present, two = 2.

**78.** Abdominal segment 2, laterotergtites [lateral view; just below spiracle]: absent = 0; present, one = 1 (Fig. 5B); present, two = 2.

**79.** Abdominal segment 3, laterotergites [lateral view]: absent = 0; present, one = 1; present, two = 2.

**80.** Abdominal segment 4, laterotergites [lateral view]: absent = 0 (Fig. 5B); present, one = 1; present, two = 2.

**81.** Abdominal segment 5, laterotergites [lateral view]: absent = 0; present, one = 1; present, two = 2.

**82.** Abdominal segment 6, laterotergites [lateral view]: absent = 0; present, one = 1; present, two = 2.

**83.** Abdominal segment 7, laterotergites [lateral view]: absent = 0; present, one = 1; present, two = 2.

**84.** Abdominal segment 8, laterotergites [lateral view]: absent = 0; present, one = 1; present, two = 2.

## Adults: body and head

**85.** Body form [dorsal view]: elongate, moderately broad = 0; broadly oval = 1; elongate, slender = 2 (Fig. 11A).

**86.** Body convexity at imaginary transverse section through basal third of elytra: very flat = 0 (Figs. 9A, 11A); moderately flat = 1; convex = 2.

**87.** Dorsal tentorial pits (or single pit, if fused) [dorsal view]: absent = 0; present = 1.

**88.** Interantennal pits [dorsal view]: absent = 0; present = 1.

**89.** Posterior part of head capsule, lateral constriction [dorsal view]: absent = 0; present = 1 (Fig. 10B).

**90.** Dorsal transverse nuchal impression [dorsal view]: absent = 0 (Fig. 9F); present = 1 (Fig. 10D).

**91.** Epistomal (= frontoclypeal) suture [dorsal view]: absent = 0 (Fig. 9F); present = 1 (Fig. 10D).

**92.** Epistomal (= frontoclypeal) suture, medial stem [dorsal view]: absent = 0 (Fig. 10O); present = 1.

**93.** Antennal insertion [dorsal view]: concealed under a ridge or a shelf-like elevation at sides of frons = 0 (Fig. 11D); fully or partly exposed = 1 (Fig. 9F).

**94.** Antennal insertion, location [dorsal view]: at, or anterior to, anterior margin of eye = 0 (Fig. 9F); posterior to anterior margin of eye = 1.

**95.** Eyes [dorsal view]: present, reduced, less than 10 ommatidia = 1; present, normal = 2.

**96.** Ommatidia structure [dorsal view]: facets hexagonal and flat, eye surface smooth = 0 (Figs. 10D, 11D); facets round and strongly convex, eye surface botryoidal = 1.

**97.** Gular sutures (or suture, if single) [ventral view]: complete, extending anteriorly to buccal cavity = 0; incomplete, obsolete in anterior 1/3 or 1/2 = 1; incomplete, obsolete in anterior 2/3, forming semicircuclar suture = 2.

**98.** Gular sutures [ventral view]: separate throughout = 0 (Fig. 11D); fused for part of their length = 1 (Fig. 10F); fused at one point = 2.

**99.** Submentum and gula [ventral view]: separated by internal ridge anterior to posterior tentorial pits = 0 (Fig. 10F); not separated by internal ridge = 1.

**100.** Tentorial bridge [ventral view]: absent = 0; present = 1 (Fig. 11D) [uninformative and deactivated].

**101.** Corporotentorium [ventral view]: present, split = 0; absent = 1; present, fused = 2 (Fig. 11D).

**102.** Anterior arms of tentorium [ventral view]: complete, reaching dorsal surface of head = 0; absent or incomplete, not reaching dorsal surface of head = 1.

**103.** Antenna [dorsal view]: not geniculate = 0 (Fig. 11A); geniculate (abruptly bent >90°) = 1 [uninformative and deactivated].

**104.** Antennomere 8 [dorsal view]: shorter and/or narrower than antennomeres 7 and 9 = 0; in sequence with length and width of antennomeres 7 and 9 = 1 (Fig. 11A).

**105.** Antennal club: absent = 0; present, gradually widening distally = 1; present, abruptly widened at base = 2.

**106.** Antennal club, proximal antennomere [dorsal view]: similar to the most of club in pubescence = 0; markedly dissimilar to the most of club, lacking most of pubescence = 1 (Figs. 9E, 10E).

**107.** Number of antennomeres in antennal club (in females, if dimorphic) [dorsal view]: zero, club absent = 0 (Figs. 10E, 11A); two or three = 1; four or more = 2 (Fig. 9E).

**108.** Labrum [dorsal view]: subquadrate to moderately transverse (≤1.5× as wide as long) = 0; strongly transverse (≥2× as wide as long) = 1 (Figs. 9K, 10J, 11E).

**109.** Labrum, whether bilobed [dorsal view]: not bilobed = 0; bilobed = 1 (Figs. 9K, 10J, 11E).

**110.** Anterior margin of labrum [dorsal view]: sclerotized at least half length = 0 (Fig. 11E); with transparent apical membrane = 1.

**111.** Anterior margin of labrum [dorsal view]: smooth = 0 (Figs. 9J, 10J, 11E); serrate = 1 [uninformative and deactivated].

**112.** Epipharynx, lateral lobes [dorsal view]: absent = 0; present, obtuse, extending slightly beyond apical margin of labrum = 1; present, acute, extending well beyond apical margin of labrum = 2 (Fig. 11E).

**113.** Split or frayed setae or setiform projections on epipharynx [ventral view]: absent = 0; present = 1.

**114.** Mandibules, length to width ratio [ventral view]: <3× = 0 (Figs. 10G, 11H); 3–5× = 1.

**115.** Mandibular apices in apposition [dorsal view]: fully exposed = 0; concealed beneath labrum = 1.

**116.** Inner edge of mandibles [ventral view]: smooth = 0 (Figs. 10G, 11H); serrate = 1.

**117.** Preapical mandibular teeth (in females, if dimorphic) [ventral view]: asymmetrical in number = 0 (Figs. 10G, 11H); symmetrical in number, or absent = 1.

**118.** Maximum number of preapical teeth on inner margin of mandibles [ventral view]: zero = 0 (Figs. 10G, 11H); one = 1; two or more = 2.

**119.** Mandibular prostheca [ventral view]: absent = 0; present = 1 (Figs. 9H, 11H) [uninformative and deactivated].

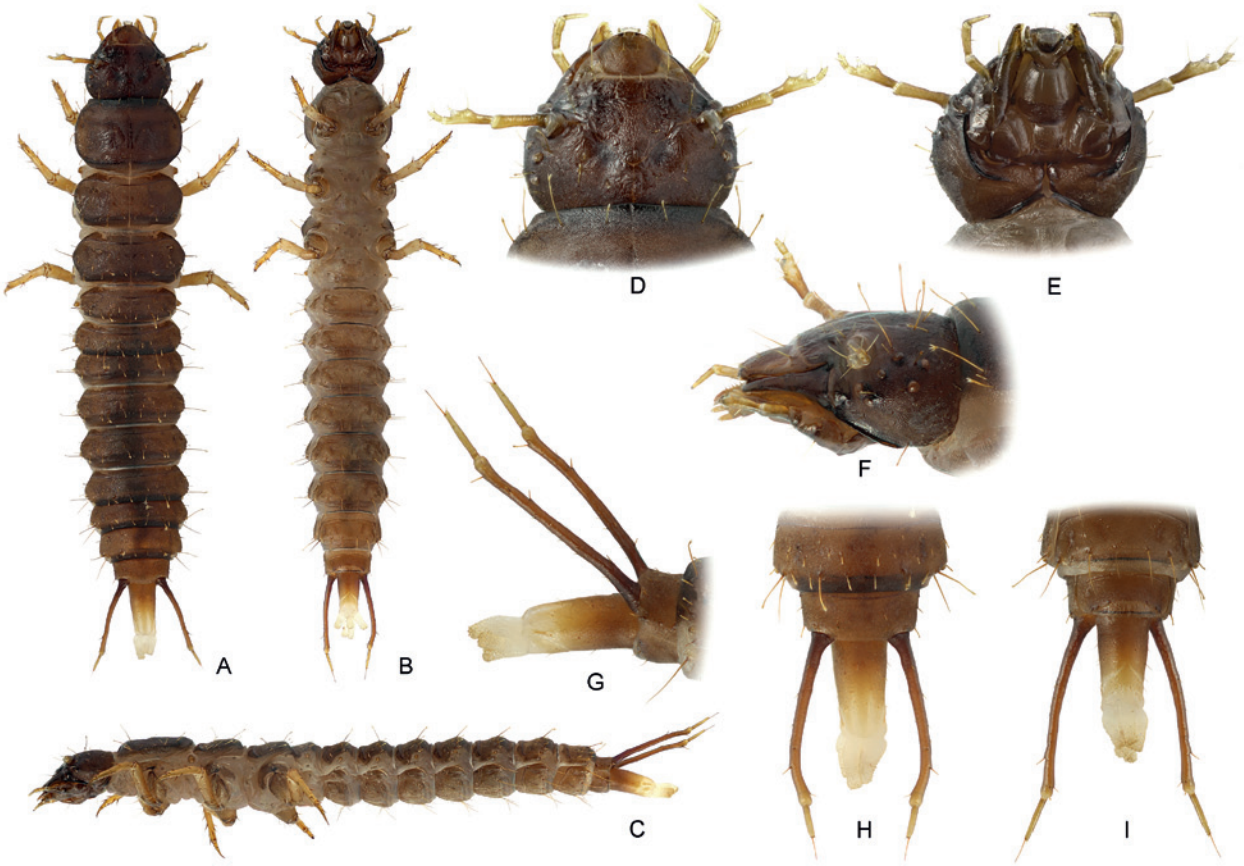


**Fig. 6.** *Nodynus leucofasciatus* (Apateticinae) larva; **A**–**C**: habitus, dorsal (A), ventral (B) and lateral (C); **D**–**F**: head, dorsal (D), ventral (E) and lateral (F); **G**–**I**: abdominal segments VIII–X, lateral (G), dorsal (H) and ventral (I). Body length 13 mm. Image author: A. Zaitsev; used with permission.

**120.** Mandibular glandular cavities on lateral surface [ventral view]: absent = 0; present = 1 [uninformative and deactivated].

**121.** Mandibular glandular cavities on baso-ventral surface [ventral view]: absent = 0; present = 1.

**122.** Mandibular glandular cavities on baso-ventral surface, number [ventral view]: one digitiform invagination = 0; pair of digitiform invaginations = 1.

**123.** Mandibular molar lobes [ventral view]: present, contiguous, well developed, with sclerotized microsculpture = 0; present, contiguous, weakly developed, with microtrichiae = 1; absent (non-contiguous) = 2.

**124.** Apical unarticulated spine of lacinia [ventral view]: absent = 0 (Fig. 10H); present = 1 (Fig. 9J).

**125.** Galea, apical setae [ventral view]: eight or more rows of fine setae = 0 (Fig. 11F); brush of setae not arranged in distinct row = 1 (Figs. 9J, 10H).

**126.** Maxillary palpomere III, length in relation to palpomere II [ventral view]: ≤0.66 = 0 (Fig. 11F); 0.8–1.2 = 1 (Fig. 10H); ≥1.4 = 2.

**127.** Maxillary palpomere IV [ventral view]: well-developed, fully sclerotized, similar in width to palpomere III = 0 (Fig. 9J); about half width of palpomere III = 1; minute, hyaline, not more that 1/4 width of palpomere III = 2.

**128.** Lateral premental lobes ("paraglossae" of some authors) [dorsal view]: absent = 0; present = 1 (Fig. 10I) [uninformative and deactivated].

**129.** Lateral premental lobes ("paraglossae" of some authors), shape [dorsal view]: broad and prominent with comb of spines and rows of fine setae = 0 (Fig. 11G); narrow with relatively few spines and setae = 1.

**130.** Medial premental lobes ("glossae" of some authors; not to confuse with lateral premental lobes or "paraglossae") [dorsal view]: absent = 0 (Fig. 9I); present = 1 (Fig. 11G).

**131.** Insertion and proximity of labial palps [ventral view]: separated by less than maximum width of basal palpomere = 0 (Fig. 9C); separated by more than maximum width of basal palpomere = 1.

**132.** Labial palpomere II [ventral view]: unmodified, subequal in width to palpomere I = 0 (Figs. 9I, 10I, 11G); strongly expanded, subglobular or subfusiform = 1 [uninformative and deactivated].

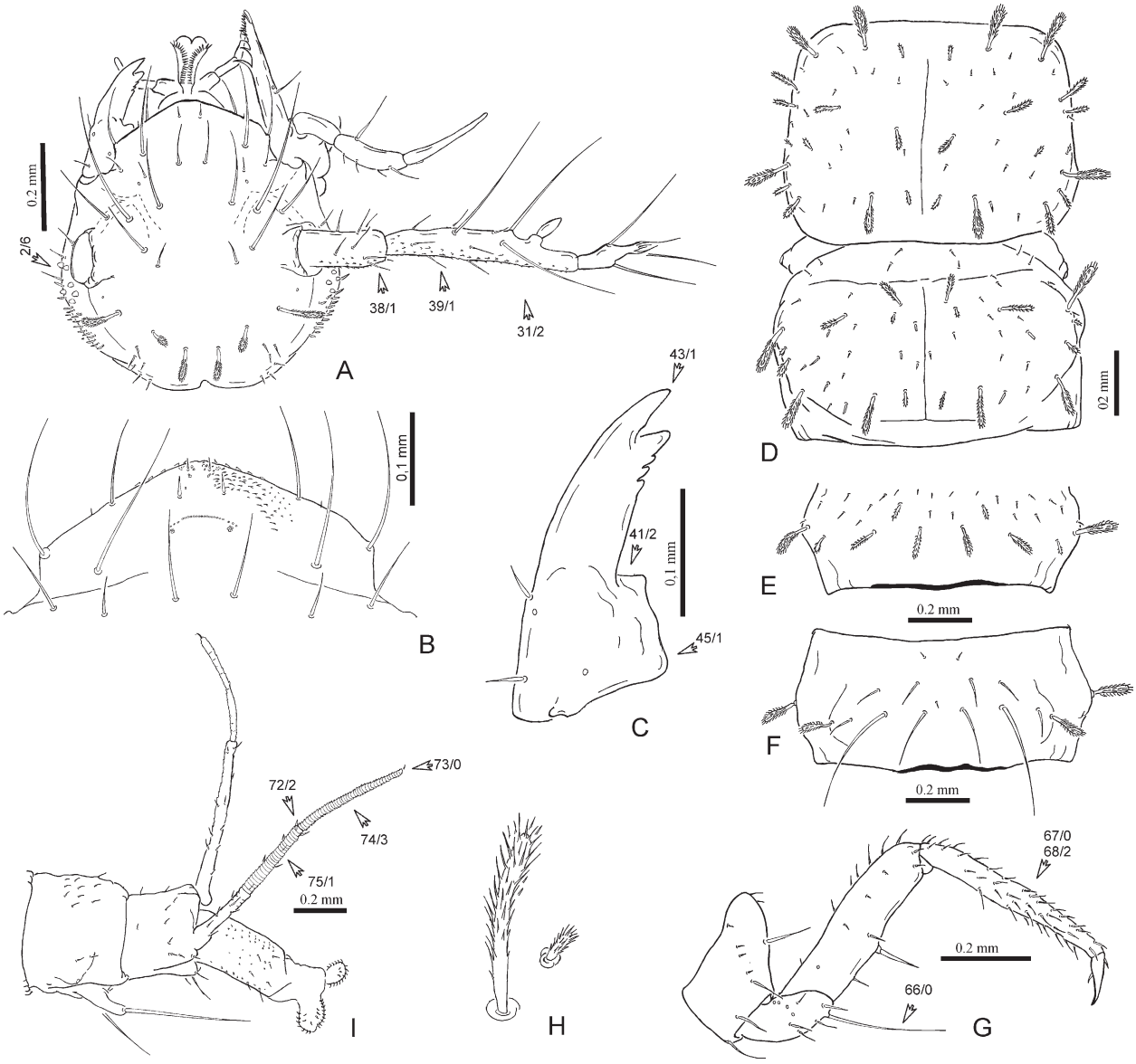


**Fig. 7.** *Trigonurus crotchii* (Trigonurinae) larva; **A**: head, dorsal; **B**: anterior part of head showing labrum partly merged with clypeus, dorsal; **C**: left mandible, dorsal; **D**: pro- and mesonotum, dorsal; **E**, **F**: abdominal segment IV, dorsal (E) and ventral (F); **G**: left fore leg, frontal; **H**: long and short frayed setae; **I**: abdominal segments VIII–X and urogomphi, left lateral.

**133.** Labial palpomere III [ventral view]: about as wide as penultimate palpomere, well sclerotized = 0 (Figs. 9I, 10I); about half as wide as penultimate palpomere, well sclerotized = 1 (Fig. 11G); acicular, hyaline, about third or less as wide as penultimate palpomere = 2; moderately to strongly expanded apically, subtriangular = 3.

**134.** Mentum [ventral view]: subquadrate or elongate = 0; transverse (≥1.5× as wide as long) = 1 (Figs. 9G, 10I).

**135.** Mentum, number of macrosetae (those ≥2× longer than surrounding ones, if any) [ventral view]: absent = 0; one pair = 1; two pairs = 2; three or more pairs = 3 (Figs. 9G, 11G).

## Adults: thorax

**136.** Cervical sclerites [ventral view]: absent = 0; slender, maximum 1/5 as wide as long = 1; robust, at least 1/4 as wide as long = 2 (Fig. 9L).

**137.** Pronotum and/or elytra, longitudinal carinae or costae [dorsal view]: absent = 0; present = 1.

**138.** Pronotum, maximal width at [dorsal view]: basal third = 0; middle or apical third = 1.

**139.** Pronotal apex (= anterior margin), width in relation to base [dorsal view]: narrower = 0; subequal = 1; wider = 2.

**140.** Pronotum, internal mid-longitudinal ridge or projection [dorsal view]: absent = 0; present,

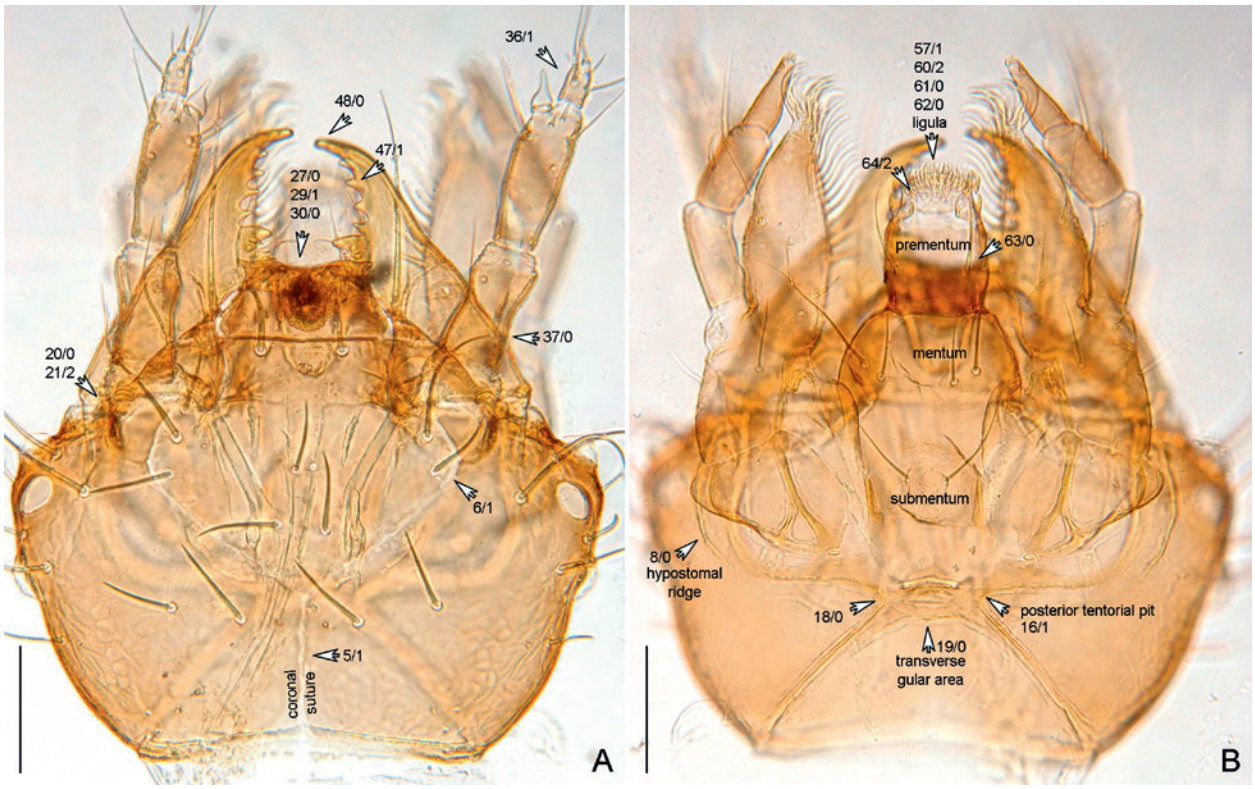


**Fig. 8.** *Bledius* sp. (Oxytelinae) larva; head dorsal (A) and ventral (B).

from single projection to short ridge less than half pronotal length = 1; present, half of pronotal length or longer = 2 (Fig. 11N).

**141.** Pair of anteprosternal plates, either small and separated or large and contiguous [ventral view]: absent = 0; present = 1 [uninformative and deactivated].

**142.** Pronotal marginal carina [lateral view]: reaching anterolateral margin without meeting notosternal suture = 0 (Fig. 10A); not reaching anterolateral margin, fused to notosternal suture = 1; obsolete anteriorly, not meeting anterolateral margin or notosternal suture = 2; absent = 3.

**143.** Inferior hypomeral marginal carina, even if incomplete [lateral view]: absent = 0; present = 1 (Fig. 9L).

**144.** Pronotum, front angles, relative to anterior margin of prosternum [ventral view]: not produced anterad = 0; produced anterad = 1 (Fig. 9L).

**145.** Pronotal hypomeron, lateral view: not inflexed, visible = 0 (Fig. 10A); inflexed, mostly not visible, except postcoxal process = 1 (Fig. 9A).

**146.** Pronotal postcoxal process of hypomeron [lateral view]: absent = 0; variously developed but weakly sclerotized, translucent, ± flexible = 1; well developed and sclerotized similarly to rest of hypomeron = 2 (Fig. 9L).

**147.** Pronotosternal suture [ventral view]: absent or very incomplete and evident only posteriorly near coxal cavity = 0; present, ± complete as fine groove or carina, not membranous = 1; present, complete, distinctly membranous = 2 (Figs. 9L, 11M).

**148.** Protrochantin [lateral view]: concealed = 0; exposed = 1 (Figs. 9L, 11M).

**149.** Protrochantin, size [lateral view]: normal = 0 (Fig. 9L); enlarged = 1 (Fig. 11M).

**150.** Anteprocoxal lobes of prosternum [ventral view]: absent = 0; present = 1 [uninformative and deactivated].

**151.** Procoxae externally [ventral view]: contiguous or subcontiguous = 0; well separated by prosternal process, even if internally subcontiguous = 1.

**152.** Prosternal process, apical shape [ventral view]: acute = 0; obtuse, rounded or truncate = 1 (Fig. 9L).

**153.** Procoxal groove articulating with ridge or tongue of prosternal process [antero-ventral view]: absent = 0; present, weakly developed, delimited by rounded carina = 1; present, well developed, delimited by sharp carina = 2.

**154.** Procoxal groove [antero-ventral view]: visible externally = 0; concealed by prosternal process = 1.

**155.** Procoxal groove, in relation to coxal length [antero-ventral view]: in apical third = 0; in median third = 1.

**156.** Procoxal cavities posteriorly [ventral view]: open = 0 (Fig. 9L); closed = 1 [uninformative and deactivated].

**157.** Procoxal cavities [ventral view]: closed internally, closure concealed = 1 [uninformative and deactivated].

**158.** Scutellum, more than half of it [dorsal view]: exposed = 0; concealed by retracted pronotum = 1.

**159.** Scutellum, transverse carina/-ae, even if strongly curved or incomplete [dorsal view]: absent = 0; present, one = 1; present, two = 2.

**160.** Elytral length relative to abdomen [dorsal view]: entire, abdomen completely concealed = 0; slightly truncate, 1–2 terga exposed = 1 (Fig. 10A); strongly truncate, 3–5 terga exposed = 2; short, 6–7 terga exposed = 3.

**161.** Elytral striation, sutural stria [dorsal view]: absent = 0; present = 1.

**162.** Elytral striation, sutural stria [dorsal view]: punctate = 0; striate = 1; punctate and striate = 2.

**163.** Elytral striation, non-sutural striae, even if reduced [dorsal view]: absent = 0; present = 1.

**164.** Elytral striation, non-sutural striae [dorsal view]: punctate = 0; striate = 1; punctate and striate = 2.

**165.** Elytral epipleural keel [lateral view]: absent = 0; present = 1 (Fig. 10A).

**166.** Subapical elytral patch of mesally- or apically-directed wing-folding spicules, underside of elytra: absent = 0; present = 1.

**167.** Elytral subapical fringe of multiple transverse rows of fine spicules, underside of elytra: absent, although scattered spicules might be present = 0; present, well-defined = 1.

**168.** Mid-lateral elytro-abdominal high friction binding patch, underside of elytra: absent = 0; present = 1.

**169.** Baso-lateral elytral patch binding with metepimeron, underside of elytra: absent = 0; present = 1 [uninformative and deactivated].

**170.** Metathoracic wings: absent or extremely reduced, non-functional = 0; present, apparently functional = 1 (Figs. 9N, 11J).

**171.** Costal hinge (= wing folding pattern) [dorsal view]: absent = 0; present = 1 (Figs. 9N, 11J).

**172.** Wing folding pattern, dorsal view: symmetrical, with about 2/3 overlap = 0; asymmetrical, with full overlap = 1.

**173.** Anal lobe (= folding part) of wing [dorsal view]: absent = 0; present = 1 (Fig. 9N).

**174.** Anal lobe of wing [dorsal view]: large (> 1/2 wing width), with small or no fringe = 0 (Fig. 9N); small (< 1/2 wing width), with long fringe = 1.

**175.** Wing venation, vein MP3: absent = 0; present = 1.

**176.** Wing venation, vein MP4: absent = 0; present = 1 (Fig. 9N).

**177.** Notch or emargination delimiting anal lobe (= folding part) of wing [dorsal view]: absent = 0; present = 1 (Fig. 9N).

**178.** Antemesosternal sclerite or sclerites [ventral view]: absent = 0; present = 1 (Fig. 9L).

**179.** Transverse mesepisternal carina, even if incomplete ("anepisternum" by NAOMI 1988: fig. 4A, Morphology Part VI) [ventral view]: absent = 0; present = 1 (Fig. 9M).

**180.** Carina delimiting prepectus from anepisternum, even if incomplete [ventral view]: absent = 0; present = 1 (Fig. 9M).

**181.** Mesoventrum, whether modified for external closure of procoxal cavities [ventral view]: not modified = 0; modified, with anterior excavation for each procoxa = 1.

**182.** Mesoventral mid-longitudinal carina [ventral view]: absent = 0; present = 1.

**183.** Mesothoracic anapleural suture, even if incomplete (NAOMI 1988: fig. 4C; Morphology part VI) [ventral view]: absent = 0; present = 1 (Fig. 9M).

**184.** Mesotrochantin [lateral view]: exposed = 0; concealed = 1 (Fig. 11I).

**185.** Mesocoxae [ventral view]: contiguous = 0 (Fig. 11I); narrowly separated by third or less coxal width = 1; widely separated by at least half of coxal width = 2.

**186.** Mesendosternites, shape [ventral view through translucent mesoventrite]: straight = 0; elbowed = 1 (Figs. 9M, 11I).

**187.** Mesendosternites, apices [ventral view through translucent mesoventrite]: free = 0; partly fused to pleural phragma = 1.

**188.** Mesendosternites, muscle disk [ventral view through translucent mesoventrite]: absent = 0; present = 1.

**189.** Mesendosternites, muscle disk, location [ventral view through translucent mesoventrite]: at apex = 0; at short anteriorly directed mid-process = 1.

**190.** Meso-metaventral suture between mesocoxae [ventral view]: absent = 0; present = 1 (Fig. 9M).

**191.** Position of meso-metaventral suture between mesocoxae in relation to coxal mid-length [ventral view]: anterior = 0 (Fig. 9M); at middle = 1; posterior = 2.

**192.** Meso-metaventral suture dorsad (above) of mesocoxae [ventral view through translucent mesocoxae]: absent = 0; present = 1.

**193.** Metaventrum, transverse carina behind mesocoxae [ventral view]: absent = 0; present, interrupted at middle = 1; present, complete = 2.

**194.** Mesal posterior lobes of metaventrum [ventral view]: absent = 0 (Fig. 9C); present = 1.


**Fig. 9.** *Necrophila americana* (Silphidae) adult; male (B, H–K, M, N, P, Q) and female (A, C–G, L, O); dorsal (E, F, I, J, K, M, N), ventral (C, G, L), frontal (D) and lateral (A, B), dorsal, ventral & lateral (H, Q, each from left to right), lateral, ventral & dorsal (O), ventral & dorsal (P); **A**, **C**: habitus; **B**: habitus, head, pronotum, and left elytron removed; **D**, **F**, **G**: head; **E**: left antenna; **H**: left mandible; **I**: labium; **J**: left maxilla; **K**: labrum; **L**: prothorax; **M**: meso- and metathorax; **N**: hind wing; **O**, **P**: abdominal apex and genitalia; **Q**: aedeagus.

**195.** Stem of metendosternite [ventral view through translucent mesoventrite]: absent = 0; present = 1 (Fig. 11I) [uninformative and deactivated].

**196.** Metacoxae, length along body's axis [ventral view]: narrowly transverse, lateral part less than half as long as longest part = 0; widely transverse, lateral part half or more as long as longest part = 1 (Fig. 11C); subconical = 2.

**197.** Posterior face of metacoxae [ventral view]: oblique = 0 (Fig. 10B); vertical = 1.

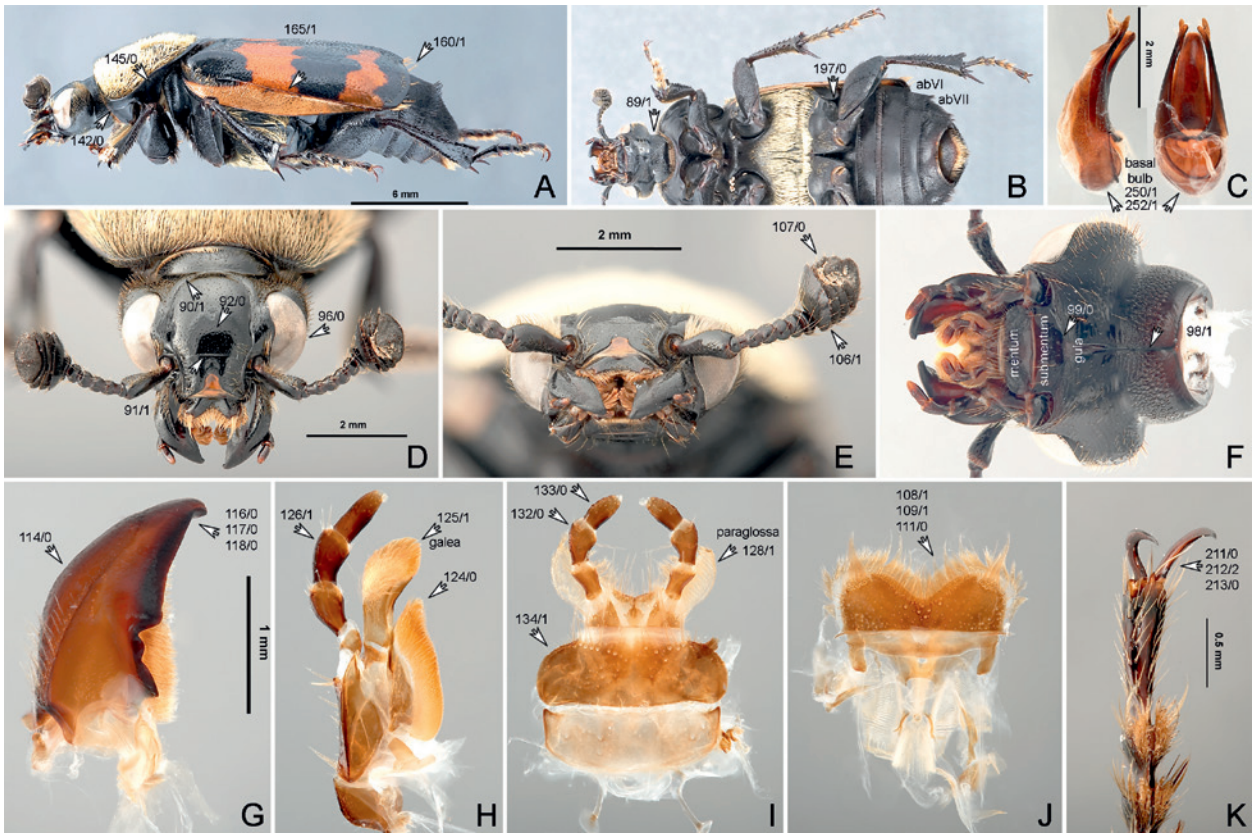


**Fig. 10.** *Nicrophorus tomentosus* (Silphidae) adult; male (C) and female (A, B, D–K); dorsal (G, H, J), ventral (B, F, I), frontal (E), lateral (A), antero-ventral (K), lateral & ventral (C). **A**, **B**: habitus; **C**: aedeagus; **D**–**F**: head; **G**: left mandible; **H**: left maxilla; **I**: labium; **J**: labrum; **K**: tarsal apex.

**198.** Mesal articulations of metacoxae with metaventrum [ventral view]: subcontiguous (separated by less than 1/10 of metacoxal width), close to mesal edges of metacoxae = 0 (Fig. 9C); widely separated (separated by more than 1/10 of metacoxal width) and on ventral side of metacoxae = 1.

**199.** Metacoxae [ventral view]: contiguous or separated by less than 1/10 of metaventral width = 0 (Fig. 9C); widely separated by more than 1/6 of metaventral width = 1.

**200.** Apical tibial spurs at least half as long as tibial width [lateral view]: absent = 0; present = 1 (Fig. 11K).

**201.** Protibia, spines along external edge [lateral view]: absent = 0; present = 1.

**202.** Protibia, rows of spines along internal edge (except, or in addition to, single row at tibial apex): absent, although non-aligned spines might be present = 0; present, one, longitudinal = 1; present, multiple, longitudinal, oblique, or transverse = 2.

**203.** Protarsal spatulate setae in males: absent = 0; present = 1.

**204.** Protarsal spatulate setae in females: absent = 0 [uninformative and deactivated].

**205.** Protarsi, number of tarsomeres, even if some connate: five = 0; four = 1; three = 2.

**206.** Protarsi, proximal tarsomeres, whether connate: not connate = 0; two connate = 1; three connate = 2.

**207.** Mesotarsi, number of tarsomeres, even if some connate: five = 0; four = 1; three = 2.

**208.** Mesotarsi, proximal tarsomeres, whether connate: not connate = 0; two connate = 1; three connate = 2.

**209.** Metatarsi, number of tarsomeres, even if some connate: five = 0; four = 1; three = 2.

**210.** Metatarsi, proximal tarsomeres, whether connate: not connate = 0; two connate = 1; three connate = 2.

**211.** Acutely rounded or apically frayed ventral process projecting between tarsal claws: absent = 0 (Fig. 10K); present = 1.

**212.** Empodial setae or setiform process: absent = 0; present, one = 1; present, two = 2 (Fig. 10K).

**213.** Tarsal claws: simple, not toothed or serrate = 0 (Fig. 10K); toothed or serrate = 1 [uninformative and deactivated].

**214.** Wing folding setal patches on tergum II [dorsal view]: absent = 0; present = 1.

**215.** Wing folding setal patches on tergum III [dorsal view]: absent = 0; present = 1.

**216.** Wing folding setal patches on tergum IV [dorsal view]: absent = 0; present = 1.
**217.** Wing folding setal patches on tergum V [dorsal view]: absent = 0; present = 1.
**218.** Wing folding setal patches on tergum VI [dorsal view]: absent = 0; present = 1.
**219.** Wing folding setal patches on tergum VII [dorsal view]: absent = 0; present = 1.

## Adults: abdomen

**220.** Fringes of fine posteriorly-directed spicules on abdominal terga [dorsal view]: absent = 0; present on one or more of terga III to V = 1.
**221.** Anterior transverse basal carina on most of abdominal terga III–VII [dorsal view]: absent = 0; present = 1 (Fig. 11B).
**222.** Basolateral ridges of abdominal terga III–V [dorsal view]: absent = 0; present = 1.
**223.** Spiracles on abdominal segment I, location [dorsal view]: in membrane beside tergum I = 0; in tergum I = 1.
**224.** Spiracles on abdominal segment II, location [dorsal view]: in membrane beside tergum II = 0; in tergum II = 1.
**225.** Spiracles on abdominal segment III, location [dorsal view]: in membrane beside tergum III = 0; in tergum III = 1.
**226.** Spiracles on abdominal segment IV, location [dorsal view]: in membrane beside tergum IV = 0 (Fig. 9B); in tergum IV = 1.
**227.** Abdominal spiracles [dorsal view]: all functional = 0 (Fig. 9B); spiracles IV to VI atrophied and non-functional = 1; spiracles IV to VII atrophied and non-functional = 2; spiracles IV to VIII atrophied and non-functional = 3.
**228.** Palisade apical fringe of microtrichia on tergum VII [dorsal view]: absent, even if some non-aligned setae present = 0; present = 1 (Fig. 11A).
**229.** Abdominal sternum III, length relative to three subsequent sterna [ventral view]: subequal to or slightly longer than (max. 1.5×) each of them = 0; about twice as long as each of them = 1.
**230.** Attachment of abdominal intersegmental membrane to preceding sternum, ventral view: apical = 0; preapical = 1.
**231.** Intersegmental membrane sclerites [ventral view]: absent = 0; present = 1.
**232.** Shape of intersegmental membrane sclerites [ventral view]: quadrangular or hexagonal, occupying >80% of membrane surface = 0; triangular or odd-angular, occupying >70% of membrane surface = 1; irregularly shaped, rounded, occupying <70% of membrane surface = 2.
**233.** Stridulatory file on each side of sternum II [ventral view]: absent = 0; present = 1.
**234.** Intercoxal carina or elevation on abdominal sterna II and III [ventral view]: absent = 0; present = 1.
**235.** Abdominal sterna II and III, metacoxal excavations [ventral view]: absent = 0; present = 1.
**236.** Lateral longitudinal carina on each side of sternum III [ventral view]: absent = 0; present = 1.
**237.** Pairs of parasclerites of abdominal segment II [lateral view]: absent = 0; one = 1; two = 2.
**238.** Pairs of parasclerites of abdominal segment III [lateral view]: absent = 0; one = 1; two = 2.
**239.** Pairs of parasclerites of abdominal segments IV–VI [lateral view]: absent = 0; one = 1; two = 2.
**240.** Pairs of parasclerites of abdominal segment VII [lateral view]: absent = 0; one = 1; two, longitudinally separated = 2; two, transversely or obliquely separated = 3.
**241.** Abdominal sterna II and III [ventral view]: solidly fused along most of their width = 0 (Fig. 9B); separated by thin membranous suture not permitting relative movement = 1; separated by long connecting membrane permitting relative movement = 2.
**242.** Tergum and sternum of abdominal segment III [lateral view]: not fused, separated by suture = 0 (Fig. 9B); fused to form complete abdominal ring = 1.
**243.** Terga and sterna of abdominal segments IV–VI [lateral view]: not fused, separated by suture = 0 (Figs. 9B, 11C); fused to form complete abdominal ring = 1.
**244.** Defensive (odoriferous) glands near abdominal apex: absent = 0; present = 1.
**245.** Structure of defensive (odoriferous) glands near abdominal apex: paired non-eversible gland reservoirs at anterior margin of tergum IX = 1; paired non-eversible pygidial glands opening into rectum = 2; unpaired gland reservoir opening externally near anus = 3; unpaired gland reservoir opening at anterior margin of sternum VIII = 4; unpaired gland reservoir opening at anterior of tergite VII = 5.
**246.** Genital segments (IX and X), eversibility: eversible to some extent (allowed by connecting membrane to VIII) = 0 (Fig. 9O); not eversible (dorsum tightly connected to underside of T VIII) = 1.
**247.** Tergum IX in male, dorsal view: entire, not divided = 0 (Fig. 9P); divided longitudinally = 1.
**248.** Terga IX and X in male [dorsal view]: not fused = 0 (Fig. 9P); fused, at least partly = 1.

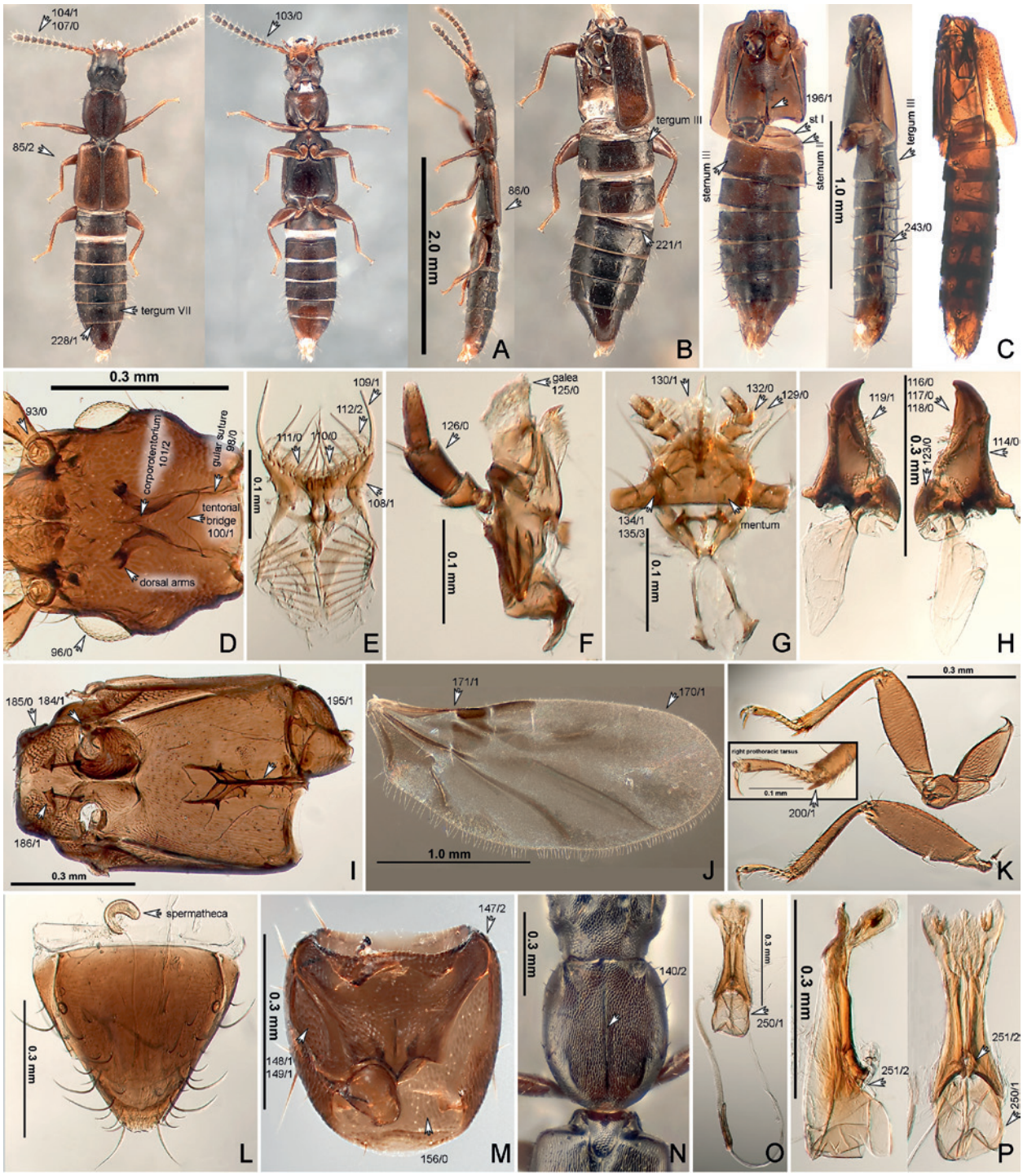


**Fig. 11.** *Renardia* sp. (Osoriinae) adult; male (A–K, N–P) and female (L, M); dorsal (B, D, E, F, I, J, L, N), ventral (G, H, M, O), dorsal, ventral & lateral (A), ventral & lateral (C), lateral & dorsal (P); **A**: habitus; **B**: habitus with head, pronotum and left elytron removed; **C**: meso-, metathorax and abdomen; **H**: head; **E**: labrum; **F**: left maxilla; **G**: labium; **H**: mandibles; **I**: meso- and metathorax; **J**: hind wing; **K**: legs; **L**: abdominal apex; **M**, **N**: pronotum; **O**, **P**: aedeagus.

**249.** Apex of sternum IX in male [ventral view]: not acutely produced (= truncate, emarginate or obtusely angulate) = 0 (Fig. 9P); acutely produced (= acuminate, or with median spiniform process) = 1.

**250.** Aedeagus, basal bulb: absent, aedeagus with large basal median foramen = 0; present, aedeagus with small subbasal median foramen = 1 (Figs. 10C, 11O, 11P).

**251.** Aedeagus, position of median foramen in re-pose (parameral side) [dorsal view]: dorsal = 0; ventral = 1; left lateral = 2 (Fig. 11P); right lateral = 3.

**252.** Aedeagus, basal piece: absent = 0; present = 1 (Figs. 9Q, 10C).

**253.** Parameres, even if markedly fused with median lobe, as in some *Pseudopsis montoraria* (Herman 1975: fig. 162): absent = 0; present = 1 (Fig. 9Q) [uninformative and deactivated].
**254.** Parameres, one or more macrosetae near apex: absent = 0 (Fig. 9Q); present = 1.
**255.** Tergum IX in females [dorsal view]: separate from tergum X = 0 (Fig. 9O) [uninformative and deactivated].
**256.** Tergum IX in female, lateral part [dorsal view]: completely separated by tergum X or connected by threadlike strip = 0 (Fig. 9O); connected by bridge at least 10% of tergal length = 1.
**257.** Female intergonopodal sclerite [ventral view]: absent = 0 (Fig. 9O); present = 1.
**258.** Gonocoxites I and II [ventral view]: distinctly separated by membrane = 0 (Fig. 9O); fused = 1.
**259.** Gonocoxites II (or gonocoxites I+II, if fused) [ventral view]: separate at midline = 0; fused = 1 [uninformative and deactivated].
**260.** Gonostyle [ventral view]: absent = 0; present = 1 (Fig. 9O).

# Appendix 2

Label data and depository information (FMNH, except as noted below) for the larvae and adults used for scoring morphological characters for the phylogenetic analysis. Only new material not previously referred to in Grebennikov & Newton (2009) is cited. Placement of taxa below subfamily (e.g., to tribe or subtribe when used) and authorship and other data about family- and genus-group names is not indicated here, but can be found, e.g., in Newton & Thayer (2005).

## Larvae

**Glypholomatinae**: *Glypholoma pustuliferum* Jeannel, 1962 (see: Thayer 2000). **Aleocharinae**: *Drusilla canaliculata* (Fabricius, 1787), Canada, Ottawa, vi.1998, V. Grebennikov (CNC). **Apateticinae**: *Apatetica* sp., P.R. China, Yunnan, Jizu Shan, 2.vii.2011, V. Grebennikov (CNC); *Nodynus leucofasciatus* (specimen depicted on Fig. 6; not studied by us), Russia, Kunashir Island, 44°16′31″N 145°56′29″E, on fermented *Betula* sap, 4.vii.2008, K. Makarov, deposited in the collection of Department of Zoology and Ecology, Moscow State Pedagogical University, Moscow, Russia. **Osoriinae**: *Renardia* sp., USA, California, Monterey Co., Los Padres N. F., Nacimiento Fergusson Rd., 28.iii.1995, A. Newton & M. Thayer; *Eleusis humilis* (Erichson, 1840), Mexico, Veracruz, Balzapote, 7.vii.1976, A. Newton; *Lispinus* sp., Panama, Canal Zone, Barro Colorado Island, 4.ii.1976, A. Newton; *Thoracophorus sculptus* Blackburn, 1902, Australia, Victoria, Mt. Margaret Rd. near Marysville, 17.ii.1993, A. Newton & M. Thayer; *Paratorchus* sp., New Zealand, Nelson Lakes N. P., 14.xii.1984–6.i.1985, A. Newton & M. Thayer; *Priochirus* sp., Mexico, Oaxaca, 15.1 mi S Valle Nacional, 14.viii.1973, A. Newton; *Glyptoma* sp., Mexico, Chiapas, Ocozocoautla, 5.ix.1973, A. Newton. **Piestinae**: *Siagonium punctatum* (LeConte, 1866), USA, Arizona, Pima Co., Mt. Lemmon, 5.ix.1974, J. Lawrence; *Hypotelus* sp., Panama, Canal Zone, Barro Colorado Island, 16–22.ii.1976, A. Newton; *Eupiestus* sp., Laos, Khammouan Pr., Ban Khoumkhan (Nahin-Nai), 4.vi.2008, A. Newton & M. Thayer; *Prognathoides mjobergi* (Bernhauer, 1920), Australia, Queensland, Lamington N. P., 25.iii.–4.iv.1985, J. & N. Lawrence. **Oxytelinae**: *Oxypius peckorum* Newton, 1982 (see: Newton 1982); *Homalotrichus* ?*nahuelbutensis* Coiffait & Sáiz, 1968, Chile, Talca Province, R. N. Altos del Lircay, 2–3.xii.2002, A. Newton & M. Thayer; *Bledius* sp., Australia, Tasmania, Crayfish Creek, 14.i.1993, A. Newton & M. Thayer; *Ochthephilus planus* (LeConte, 1866), USA, New Hampshire, Coos Co., 0.7 mi S Jefferson Notch, 31.vii.1982, A. Newton & M. Thayer; *Anotylus rugosus* (Fabricius, 1775), Canada, Ottawa, iv.1998, V. Grebennikov (CNC). **Scaphidiinae**: *Scaphium castanipes* Kirby, 1837, USA, New Hampshire, Coos Co., 0.7 mi S Jefferson Notch, 17.ix.1983, A. Newton & M. Thayer; *Scaphisoma* sp., USA, New Hampshire, Coos Co., Pine Mt., 27.vii.1974, A. Newton; *Cyparium terminale* Matthews, 1888, Mexico, Tenancingo, 11.ix.1973, A. Newton; *Scaphidium geniculatum* Oberthur, 1884, Panama, Cerro Azul, 22.vi.1976, A. Newton.

## Adults

**Glypholomatinae**: *Glypholoma pustuliferum* Jeannel, 1962, Chile, Malleco Pr., 20 km E Manzanar, 1100 m, 19–31.xii. 1976, S. Peck. **Aleocharinae**: *Drusilla canaliculata* (Fabricius, 1787), Bosnia-Hercegovina, no date, K. Brancsik. **Apateticinae**: *Apatetica princeps* (Sharp, 1874), Japan, Saragamine Iyo, 5.vii.1953, T. Mohri. **Osoriinae**: *Renardia* "*nigrella*" (LeConte, 1863), USA, California, El Dorado Co., Blodgett Forest, 28.iv.1976, A. Newton; *Eleusis humilis* (Erichson, 1840), Panama, Canal Zone, Barro Colorado Island, 16–22.

ii.1976, A. Newton; *Lispinus* sp., Panama, Canal Zone, Barro Colorado Island, 4.ii.1976, A. Newton; *Thoracophorus sculptus* Blackburn, 1902, Australia, Victoria, Acheron Gap, 28–30.iv.1978, S. Peck; *Paratorchus hamatus* McColl, 1982, New Zealand, BR, Lake Rotoiti, 6.ii.1978, S. & J. Peck; *Priochirus bicornis* (Fauvel, 1864), Mexico, Hidalgo, 3.2 mi N Tlanchinol, 6.vii.1973, A. Newton; *Glyptoma* sp., Panama, Canal Zone, Barro Colorado Island, vii.1969, J. Lawrence & T. Hlavac. **Piestinae**: *Piestus minutus* Erichson, 1840, Panama, Canal Zone, Barro Colorado Island, 16–22.ii.1976, A. Newton; *Hypotelus* sp., Panama, Canal Zone, Barro Colorado Island, 16–22.ii.1976, A. Newton; *Eupiestus* sp., Laos, Khammouan Pr., Ban Khoumkhan (Nahin-Nai), 4.vi.2008, A. Newton & M. Thayer; *Prognathoides mjobergi* (Bernhauer, 1920), Australia, Queensland, Lamington N. P., 25.iii.–4.iv.1985, J. & N. Lawrence. **Oxytelinae**: *Oxypius peckorum* Newton, 1982, Australia, Western Australia, Walpole N. P., 18–27.vi.1980, S. & J. Peck; *Homalotrichus* ?*nahuelbutensis* Coiffait & Sáiz, 1968, Chile, Malleco Pr., Malalcahuello, 30 km E Curacautin, 1100 m, 19–31.xii.1976, S. Peck; *Bledius* sp., USA, California, Del Norte Co., 6 mi SE Smith River, 3–5.vii.1975, A. Newton & M. Thayer; *Ochthephilus columbiensis* (Hatch, 1957), USA, Oregon, Clackamas Co., 1.5 mi S junction US26 & Oregon35, 11.vii.1975, A. Newton & M. Thayer; *Anotylus rugosus* (Fabricius, 1775), Bosnia-Hercegovina, no date, K. Brancsik. **Scaphidiinae**: *Scaphium castanipes* Kirby, 1837, USA, Alaska, Fairbanks Univ. Boreal Arboretum, 9.viii.1984, S. & J. Peck; *Scaphisoma commune* Löbl, 1997, USA, California, Amador Co., Peddler Hill, 7000 ft., 27.vi.1975, A. Newton & M. Thayer; *Cyparium* sp., South Africa, Natal, Cathedral Peak, 75 km WSW Estcourt, 2000 m, 7–31.xii.1979, S. & J. Peck; *Scaphidium quadriguttatum* Say, 1823, USA, Massachusetts, Middlesex Co., Estabrook Woods, near Concord, 4.vii.1974, A. Newton.

# Appendix 3

## Description and diagnosis of *Apatetica* larva

Fig. 5

**Description.** Frayed setae present on body; body sclerites, urogomphi and legs with markedly developed toothed microsculpture. **Head capsule** with 6 stemmata; about 0.9× as wide as prothorax; coronal suture 0.4× length of head capsule (Fig. 5F); dorsal ecdysial lines Y-shaped with maximal width between apices; hypostomal ridge near maxillary foramina present, not reaching posterior tentorial pits; posterior tentorial arms present, extending inside head capsule and joined with thin tentorial bridge; posterior tentorial arms arise from, and connect with the rest of tentorium, relatively wide, not more than 20× as long as wide; tentorial bridge present, arises from posterior tentorial arms; posterior tentorial pits curved in shape, not touching each other with distance between them not greater than width of widest maxillary palpomere; corporotentorium (Fig. 5N) inside head capsule and connected to ventral wall with ventral arms; co-joining ventral edges of epicranial plates subequal to or longer than length of prementum; gula absent; dorsal mandibular articulation separated from antennal membrane by sclerotized strip as wide as width of antennomere 1; internal transverse ridge formed by anterior tentorial arm attachment present, long, straight; labrum separated from clypeus by distinct suture visible for entire length; each side of labrum near its articulation to clypeus with 2 lateral sclerites; anterior edge of labrum even, not toothed or serrate, noticeably convex, without distinct median tooth. **Antennae** with 3 antennomeres, about as long as head capsule (Fig. 5H); antennomere 1 about 2–3× as long as wide; main sensory appendage on antenna anterior/mesal with respect to articulation of antennomere 3, bulbous or conical, with convex sides, shorter than width of antennomere 2 (Fig. 5G); antennomere 3 of regular shape, ratio length to width 2–3×; antennomere 1 not constricted or interrupted by membrane, without setae; antennomere 2 with 3 long setae; apical half of antennomere 3 with 3 long setae (excluding a single non-articulated seta-like sensory structure). **Mandibles** with smooth or obtuse angle of medial outline between widened basal and narrowed apical parts (Fig. 5K); with subapical tooth in apical quarter (Fig. 5K); apices acutely pointed; mola absent; mandibular width at base 2× to that at middle; symmetrical or almost symmetrical; mesal mandibular serration apparently absent (Fig. 5K) or extremely minute and distinguished only under high magnification; mandibles slightly curved, apices when open directed anteriorly; mesal mandibular profile not sickle-shaped. **Ventral mouthparts**: cardo with transverse ridge on its sclerotized part; galea and lacinia completely fused along entire length forming mala widest at base (Fig. 5L); maxillary palpomere 1 (the one apicad of maxillary palpifer) equal to or shorter than 0.8× length of maxillary palpomere

2; maxillary palpomere 2 with 2 setae; maxillary palpomere 3 without setae; sclerotization on mentum and submentum distinct and separated by membrane; submentum laterally free from head capsule; ligula present, about as long as wide, markedly (≥ 2 ×) wider than basal labial palpomere; ligula tetra-lobed (Fig. 5M); ventral sclerite of prementum indistinctly sclerotized or, if distinct, then entire; labial palpi separated by more than 1.5 × palp width. **Thorax and abdomen**: cervicosternum (= eusternum) subdivided, consisting of several sclerites; trochanter with the leg's longest seta; tibiotarsus not widened at middle, with less than 10 setae; abdomen evenly narrowing posteriad, without lateral tergal lobes extending laterally and overhanging body sides; pygidium (segment X) distinctly longer than wide; urogomphi 1-segmented; long apical seta on urogomphi (at least 25% urogomphal length) absent; urogomphi ≥ 3 × as long as tergum VIII, with ring-shaped microsculpture; abdominal sclerites clearly distinguishable from surrounding membrane; abdominal segments 1 – 3 each with 1 laterotergite per side; abdominal segments 4 – 9 without laterotergites.

**Diagnosis.** From similar larvae of the most closely related *Nodynus* (Fig. 6) those of *Apatetica* differ by having antennae about as long as head capsule (noticeably shorter in *Nodynus*, Fig. 6D); abdomen evenly narrowing posteriad (parallel-sided most of its length in *Nodynus*, Fig. 6A,B); urogomphi 1-segmented (2-segmented in *Nodynus*, Fig. 6H,I).